Linköping Studies in Science and Technology
Dissertation No. 1948

ON THE PERFORMANCE OF STRATIFIED VENTILATION

ULF LARSSON

Division of Energy Systems
Department of Management and Engineering
Linköping University, SE-581 83 Linköping, Sweden

2018

“On the performance of Stratified Ventilation”

Linköping Studies in Science and Technology, Dissertation No. 1948

ISBN: 978-91-7685-251-4
ISSN: 0345-7524

Printed in Sweden by LiU-Tryck, Linköping, 2018.

Distributed by:
Linköping University
Department of Management and Engineering
SE-581 83 Linköping, Sweden
Tel: +46 13 281000

Abstract

People nowadays spend most of their time indoors, for example in their homes, cars, in trains, at work, etc. In Sweden, the energy demand in the built environment is a growing issue. The building sector accounts for 40% of total energy use and 15% of total CO_2 emissions, and around one-third of the energy use in the world is related to providing a healthy and good comfort indoors. To achieve acceptable indoor climates new designs for the ventilation systems have been proposed in recent decades, among them stratified ventilation systems.

Stratified ventilation is a concept that often allows good performance for both indoor air quality and thermal comfort. Stratified ventilation systems are effective in reducing cross contamination, since there is virtually no mixing in the space; the temperature and the pollutant concentration increase linearly from the heat source with the height of the occupied zone. There are many different ventilation supply devices using the stratified principle, such as displacement supply device (DSD), impinging jet supply device (IJSD) and wall confluent jet supply device (WCJSD).

The main aim of this thesis is to analyze and compare different supply devices based on stratified ventilation, with different setups, related to thermal indoor climate, energy efficiency and ventilation efficiency. The ultimate goal is to contribute to an increased understanding of how ventilation systems with stratified supply devices perform.

Two scientific methods have mainly been used in this thesis, i.e., experimental and numerical investigations. For numerical experiments the CFD (Computational Fluid Dynamics) code ANSYS and FIDAP have been used. Experimental studies have been performed with thermocouples, Hot-Wire Anemometry (HWA) and Hot-Sphere Anemometry, thermal comfort measurement equipment and tracer gas measurement equipment.

This thesis mainly focuses on three research questions: Interaction between a supply device based on stratified ventilation and downdraft from windows; Flow behavior, energy performance and air change effectiveness for different supply devices based on stratified

ventilation; and Thermal comfort for different supply devices based on stratified ventilation.

Research question one showed that the arrangement of displacement supply device and window in cold climate has significant effect on the flow pattern below the window. Different supply airflow rates have an effect on both the velocity and the temperature of the downdraft. In this case the velocity decreased by approximately 9.5% and the temperature in the downdraft decreased 0.5°C when the flowrate from the supply device increased from 10 to 15 l/s.

Research question two showed that airflow patterns between different air supply systems were essentially related to characteristics of air supply devices, such as the type, configuration and position, as well as air supply velocities and momentum. For WCJSD, IJSD and DSD, positions of heat sources (such as occupant, computers, lights and external heat sources) played an important role in formation of the room airflow pattern. One interesting observation is that the temperature in the occupied zone is lower and a more stratified temperature field implies a more efficient heat removal by a stratified air supply device. The results revealed that the lowest temperature in the occupied zone was achieved for DSD, but with IJSD and WCJSD slightly warmer, while the system with a mixing supply device (MSD) showed a much higher temperature. The results confirm that air change effectiveness (ACE) for the DSD, WCJSD and IJSD is close to each other. However, MSD shows lower ACE in all the present papers than IJSD, WCJSD and DSD.

Research question three showed that ventilation systems with stratified supply devices in almost all of the studied cases showed an acceptable level for predicted percentage dissatisfied (PPD), predicted mean vote (PMV) and percentage dissatisfied due to draft (DR). If comparing ventilation systems, using IJSD, WCJSD or DSD with MSD always showed thermal comfort better or at the same level.

Sammanfattning

Människor spenderar en stor del av sin tid inomhus, exempelvis i sina bostäder och bilar, på tåg och på arbetet. Sveriges energibehov i den byggda miljön har en växande trend. Byggnadssektorn står för 40 % av det totala energibehovet och för 15 % av CO_2 utsläppet och för cirka en tredjedel av energianvändningen i världen för att tillhandahålla en hälsosam och bra inomhusmiljö. För att skapa en bra inomhusmiljö har nya sätt att ventilera inomhusmiljön utvecklats under de senaste årtiondena. De olika principer som används för att ventilera en byggnad kan indelas i: kolvströmning, omblandande strömning och deplacerande strömning. De genererar rumsförhållanden som ger olika fördelning av hastighet, temperatur och föroreningar i det ventilerade utrymmet.

Stratifierad ventilation är ett koncept som ofta ger ett bra utfall av både inomhusluftkvalitet och termisk komfort. Stratifierade system är effektiva för att minska korskontaminering, eftersom det nästan inte finns någon omblandning i rummet, temperaturen och föroreningskoncentration ökar linjärt från värmekällan med höjden i vistelsezonen. Det finns många olika ventilationsdon som använder den stratifierade principen, såsom deplacerande ventilationsdon (DSD), impinging jet-ventilationsdon (IJSD) och väggbaserad confluent jet-ventilationsdon (WCJSD).

Huvudsyftet med denna avhandling är att analysera och jämföra olika tilluftsdon baserat på stratifierad princip i olika rumskonfigurationer med avseende på termiskt inomhusklimat, energieffektivitet och ventilationseffektivitet. Det yttersta målet är att bidra till ökad förståelse för hur ventilationssystem med olika stratifierade tilluftsdon fungerar.

Två vetenskapliga metoder har huvudsakligen använts i denna avhandling: experimentella och numeriska analyser. För numeriska analyser har CFD (Computational Fluid Dynamics) använts. De simuleringsprogram som utnyttjats för detta ändamål är ANSYS och FIDAP. Experimenten har utförts med hjälp av termoelement, varmtråds- och varmsfärsteknik, mätutrustning för termisk komfort och mätutrustning för spårgas.

Denna avhandling fokuserar framför allt på tre forskningsfrågor: interaktion mellan ett tilluftsflöde från ett deplacerande don och kallraset från ett fönster; strömningsbilden, energiprestandan och luftbyteseffektiviteten för olika tilluftsdon baserat på stratifierad ventilation; och termisk komfort för olika tilluftsdon baserade på stratifierad ventilation.

Forskningsfråga ett visade att kombinationen av tilluftsflöde genom ett deplacerande don och fönster i kallt klimat har tydlig effekt på strömningsbilden för kallraset under fönstret. Olika tilluftsflöden har en effekt på både hastigheten och temperaturen i kallraset. I detta fall minskade hastigheten med ca 9,5% och temperaturen i kallraset minskade med 0,5°C när flödeshastigheten från tilluftsdonet ökade från 10 till 15 l/s.

Forskningsfråga två visade att luftflödesmönstren mellan olika luftförsörjningssystem väsentligen var relaterade till egenskaper hos tilluftsdonen, såsom typ, konfiguration och position samt lufttillförselhastigheter och impulskraft. För WCJSD, IJSD och DSD spelade värmekällans placering, d.v.s. människor, datorer, belysning och externa värmekällor, en viktig roll vid utformningen av rummets luftflödesmönster. En intressant observation är att temperaturen i vistelsezonen är lägre och rummet har ett mer stratifierat temperaturfält, vilket innebär en effektivare ventilering av den zonen. Resultaten visade att den lägsta temperaturen i vistelsezonen uppnåddes för DSD medan IJSD och WCJSD visade en något högre temperatur, systemet med ett omblandande don (MSD) visade en påtagligt högre temperatur. Resultaten bekräftar också att luftförändringseffektiviteten (ACE) för DSD, WCJSD och IJSD ligger nära varandra. MSD visar dock i alla ingående artiklar lägre ACE än IJSD, WCJSD och DSD.

Forskningsfråga tre visade att ventilationssystem med stratifierade tilluftsdon i nästan samtliga studerade fallen haren acceptabel nivå för predicted mean vote (PPD), predicted mean vote (PMV) och percentage dissatisfied due to draft (DR). Om man jämförde ventilationssystem IJSD, WCJSD eller DSD med MSD visade det sig alltid att den termiska komforten var bättre eller på samma nivå som för MSD.

Acknowledgements

I thank my supervisor Professor Bahram Moshfegh with all my heart, for valuable guidance, encouragement and support during the development of this work. Thank you too for your patience with being my supervisor, but in all these years we worked together, our roles have evolved into more than a professional relationship, nowadays I consider us close friends.

During almost all of my work, a person has always been close to me, he has contributed scientific help, companionship and contributed to the fact that I feel so comfortable at the University of Gävle. Thanks, Mathias Cehlin.

I really want to thank Associate Professor Taghi Karimipanah, for our discussions and for your advice. I also want to thank Professor Mats Sandberg who was involved in my licentiate degree, some papers from that work are now a part of my thesis. Thanks also to Professor Hazim Awbi who has read my thesis and given me many good suggestions to improve it.

Other people I want to thank are, Elisabet Linden, Hans Lundström and Claes Blomqvist who have contributed to my work as part of this thesis. A special thanks to Arman Ameen for his helps with some figures, especially the figure on the cover page. I would also like to thank all the other people at the lab that helped me during these years.

In order to complete this work while having other tasks in the department, it is necessary to have understanding heads and therefore I would like to thank my current head of faculty Gunilla Mårtensson and my former head of faculty Bengt Eriksson. I would also like to thank Eva Wännström for helping me administratively in my job as head of department, which made it possible for me to complete my assignment.

Finally, I want to thank my wife, Marie, deeply. She's the one who listened to me when I have talked about this thesis. I'm forever grateful that you did not get tired of me.

List of publications

The present doctoral dissertation is based on the following papers:

Paper I:

Larsson, U., Moshfegh, B. and Sandberg, M. (1999). Thermal analysis of super insulated windows (numerical and experimental investigations). *Energy and Buildings*, 29, pp. 121-128.

Paper II:

Larsson, U. and Moshfegh, B. (2002). Experimental investigation of downdraught from well-insulated windows. *Building and Environment*, 37*,* pp. 1073-1082.

Paper III:

Chen, H. J., Janbakhsh, S., Larsson, U. and Moshfegh, B (2015). Numerical investigation of ventilation performance of different air supply devices in an office environment. *Building and Environment*, 90*,* pp. 37-50.

Paper IV:

Arghand, T., Karimipanah, T., Awbi, H., Cehlin, M., Larsson U. and Linden, E. (2015). An experimental investigation of the flow and comfort parameters for under-floor, confluent jets and mixing ventilation in an open-plan office. *Building and Environment*, 92*,* pp. 48-60.

Paper V:

Larsson, U. and Moshfegh, B. (2017). Comparison of ventilation performance of three different air supply devices: a measurement study. *International Journal of Ventilation*, 16 (3)*,* pp. 244-254.

Paper VI:

Cehlin, M., Larsson, U., and Chen, H. (2018). Numerical investigation of air change effectiveness in an office room with impinging jet ventilation. In Proc. of COBEE 2018 – 4th International Conference on Building Energy and Environment, pp. 641-646.

Paper VII:

Larsson, U. and Moshfegh, B. (2018). Comparison of the thermal comfort and ventilation effectiveness in an office room with three different ventilation supply devices - a measurement study. In Proc. of 14th International Conference of Roomvent & Ventilation, pp. 187-192.

The following papers were published but they are not included in this thesis:

Larsson, U., Moshfegh, B., and M. Sandberg, *Natural Convection within a Rectangular Enclosure in a Window Construction*, Proceedings of the CIB World Building Congress, Symposium B, pp. 1303-1311, June 7-12, 1998, Gävle, Sweden.

Larsson, U., and Moshfegh, B. *Effect of Window Bay on the Downdraught from a Well-Insulated Window*, Proceedings of the Roomvent 2000 congress, July 9-12, 2000, Reading, United Kingdom, Vol. 2, pp. 773-781.

Cehlin, M., Moshfegh, B., Karlsson, F., and Larsson, U. (2008). Analysis on Thermal Comfort for a Hospital Building by Multi-zone Modeling: Summer Condition. In *World Renewable Energy Congress X, 19-25 July, 2008, Glasgow, Scotland*.

Karimipanah, Taghi, Ulf Larsson, and Mathias Cehlin. "Investigation of flow pattern for a confluent-jets system on a workbench of an industrial space." *13th International Conference on Indoor Air Quality and Climate, July 7-12, 2014, Hong Kong*. 2014.

Cehlin, Mathias, Taghi Karimipanah, and Ulf Larsson. "Unsteady CFD simulations for prediction of airflow close to a supply device for displacement ventilation." *13th International Conference on Indoor Air Quality and Climate, Indoor Air 2014, 7-12 July 2014, Hong Kong*. 2014.

Larsson, Ulf, and Bahram Moshfegh. "Comparison of ventilation performance of three different air supply devices-A measurement study." *11th International Conference on Industrial Ventilation, Ventilation 2015, 26-28 October 2015, Shanghai, China*. Vol. 1. International Conference on Industrial Ventilation, 2015.

NOMENCLATURE

C_n : Number (n) of coefficients in turbulence models, (-)
c_p : Specific heat at constant pressure, (J/kg·°C)
F_1 : Blending function, (-)
f : Elliptic relaxation factor, (-)
g : Gravity, (m/s^2)
k : Thermal conductivity, (W/m·°C)
: Turbulent kinetic energy, (m^2/s^2) and Number of factors, (-)
l : Length scale, (m)
M : Metabolism, (W/m^2)
P : Pressure, (Pa)
Pr : Prandtl number, (-)
Re : Reynolds number, (-)
T : Turbulent time scale, (s)
: Temperature, (°C)
T_u : Turbulence intensity, (-)
T_a : Air temperature, (°C)
U : Mean velocity, (m/s)
$U_i = (U, V, W)$: Mean velocity component, (m/s)
u : Velocity, (m/s)
$u_i = (u, v, w)$: Instantaneous velocity component, (m/s)
u_τ : Friction velocity, (m/s)
u' : Fluctuating velocity, (m/s)
$u_i' = (u', v', w')$: Fluctuating velocity component, (m/s)
v_{ar} : Relative air velocity, (m/s)
$\overline{v^2}$: Wall normal Reynolds stress component, (m^2/s^2)
$x_i = (x, y, z)$: Cartesian coordinate, (m)
S_m, S_θ : Source terms (N/m^3) and (W/m^3) respectively
y : Normal distance to the wall, (m)
y^+ : Dimensionless distance from the wall, (-)

Greek symbols

α	: Thermal diffusivity, (m^2/s) and Relaxation factor, (-)
β	: Volumetric thermal expansion coefficient, (1/K)
δ_{ij}	: Kronecker delta function, (-)
ε	: Rate of dissipation of turbulent kinetic energy, (m^2/s^3)
ε_t	: Heat removal effectiveness, (-)
ε_a	: Air exchange efficiency, (-)
ε_p^a	: Local air change index, (-)
ϕ	: General scalar variable, (-)
μ	: Dynamic viscosity, (kg/m·s)
μ_t	: Turbulent viscosity, (kg/m·s)
ν	: Kinematic viscosity, (m/s^2)
Θ	: Time averaged temperature, (°C)
θ	: Instantaneous temperature, (°C)
θ'	: Fluctuating temperature, (°C)
ρ	: Density, (kg/m^3)
σ_k, σ_ε, σ_t	: Turbulent Prandtl number, (-)
τ_a	: Actual air change rate (s)
τ_n	: Nominal time constant (s)
τ_w	: Wall shear stress, (N/m^2)
$\{\overline{\tau}\}$	: Mean age of air (s)

Abbreviations

ACE	: Air change effectiveness
CFD	: Computational fluid dynamics
CT	: Constant temperature
CPU	: Central processing unit
DR	: Draught rating
DSD	: Displacement supply device
FEM	: Finite element method
FVM	: Finite volume method

GDP : Gross domestic product
GHG : Greenhouse gas
HWA : Hot wire anemometry
IJSD : Impinging jet supply device
LES : Large eddy simulation
MAA : Mean age of air
MSD : Mixing supply device
PMV : Predicted mean vote
PPD : Predicted percentage dissatisfied
SBS : Sick building syndrome
UFAD : Under floor air distribution
UFASD : Under floor air distribution supply device
WCJSD : Wall confluent jet supply device
WCJV : Wall confluent jet ventilation

Table of Contents

1 Introduction

The main function of buildings is to act as a protection against the outdoor environment and to provide a healthy indoor climate. Not long ago and still in a number of countries, the provision of good indoor climate was or remains rather low. However, many countries today have increased the demands for proper indoor climate to a high level that includes the provision of thermal comfort, lighting, noise reduction, etc. The requirements for indoor climate depend on who or what will spend time in the indoor climate and/or what activity is taking place. People's demands are often related to thermal comfort or indoor air quality.

People nowadays spend most of their time indoors, whether at home, commuting, at work, etc. In Sweden, the energy demand in the built environment is a growing issue. The building sector accounts for 40% of total energy use and 15% of total CO_2 emissions, and around one-third of the energy use in the world is related to providing a good and healthy indoor environment. Since many countries in the EU already have achieved the goal for 2020 (reduce greenhouse gas (GHG) emissions by 20%, see (Anger and Zannier, 2017), the focus for EU now is to reduce energy use and GHG emissions by 40% by 2030 and by 80 – 95% by 2050.

One of the priority areas for achieving these goals is applying energy efficiency measures in buildings. To achieve an acceptable indoor climate with consideration for thermal comfort and air quality, most buildings have some kind of air exchange with the surroundings, mainly forced air exchange but also natural air exchange. The magnitude of the air exchange rate is often one of the important parameters influencing people's experience of the indoor climate. Perception of indoor climate has also been an important societal issue with consideration for people's well-being, productivity, learning, etc. One way is to build passive houses but research shows that there are several parameters that affect how this energy-saving measure affects the result of indoor climate (Brunsgaard *et al.*, 2012).

The oil crises of the 1970s raised awareness of energy use in buildings, which contributed to changes in the envelope of buildings to

save energy. The walls, roofs and floors became more insulated and air leakage tightened. In the same spirit the air exchange rate was also reduced. The result of these changes, however, created dissatisfaction with the indoor climate and cases of "sick building syndrome" (SBS) (Skov, Valbjørn and Pedersen, 1990; Wargocki et al., 1999).

Poor indoor climate has also affected people's productivity (Jaakkola, Heinonen and Seppänen, 1989; Fisk and Rosenfeld, 1997; Wyon, 2004). Good indoor climate has a significant positive influence on work performance, and in contemporary society, when people spend most of their time indoors, the quality of the indoor climate has a major influence on a country's GDP.

To achieve acceptable indoor climate, new designs for ventilation systems have been proposed in recent decades. The natural ventilation systems have been altered with mechanical ventilation systems where the airflow and temperature inside the building are controlled for the purpose of attaining good comfort with an acceptable energy use. Other advantages with mechanical ventilation are the possibilities to recover heat from the exhaust air and also advantages of cleaning of the supply airflow.

New ventilation concepts are being proposed with the intention of achieving good indoor air quality and thermal comfort. The principles of airflow distribution in buildings are divided into three types: piston flow, mixing flow, and stratified flow. They generate room conditions that lead to differences in the distribution of velocity, temperature, and contaminants in the ventilated space.

Windows are one of the parts of the building shield that have a significant influence on the indoor climate. The temperature difference between the inner surface of the window pane and indoor temperature creates movements of the air that can be perceived as an uncomfortable draft (Heiselberg, 1994). As a result, different types of heating and ventilation systems have been used to prevent this draft from penetrating into the occupied zone of the room. In recent decades the construction of windows has been developed to facilitate other designs of heating and ventilation systems.

1.1 Challenges of Stratified Ventilation

Performance of ventilation systems is influenced to a great extent by forces generated in the room from heat sources (machines, people, computers, lighting, etc.) and downdraft from cold surfaces (windows). In addition, the room configuration has a major influence on the efficiency of the ventilation systems.

Downdraft from cold windows is a force that will disturb or strengthen the flow path from the ventilation devices. For example, flow from a displacement device can collide with a downdraft from a window during winter, but in the summer the flow created from the windowpane is more or less absent or has a different direction.

How stratified ventilation systems perform, e.g. in offices, depends on many parameters such as the design of the offices (single room or open plan), and how they are equipped with heat sources such as computers, printers, furniture, etc. In addition, where people are stationed in the room and how they normally move around has an influence on the performance of the ventilation system in the room. As a result, stratifying ventilation systems have a rather complex flow feature; the airflow pattern is unsteady and varies when people or other heat sources move around in the room.

Ventilation systems used for cooling often have a problem with comfort because of the cold airflows from the supply device. The idea of stratified ventilation is to deliver air directly to the zones where cooling is needed, i.e., to areas where occupants or other heat sources are located. Mixed ventilation systems cool by rapidly lowering the average temperature in the room by blending, while stratified ventilation delivers the supply air directly to the area where the heat source is located without any major interference with the room air. Either way, it produces a temperature profile that has a relatively low temperature and high speed at the floor level which can cause discomfort in some areas of the room. If the ventilation system is also used to heat the air during certain times of the year, hot plumes will rise instead, and then the problem of comfort is almost gone, but in return, the power created by gravity changes and, consequently, the performance of the ventilation system is altered. Stratified ventilation systems usually use the room's surfaces when transporting air jets into

the room, which in certain environments can cause problems. For example, furniture or other obstacles in the room can disturb the intended path of the air movement, which can cause undesired effects such as unventilated areas.

1.2 Objective

With regard to what has been mentioned above, it is important from many aspects to improve the performance of stratified ventilation to make it more efficient. One important aspect is to reduce the energy use by the ventilation system as it has a major impact on a building's energy performance. However, it is also important to highlight that the main task for a ventilation system is to provide an indoor climate that is healthy and has a thermal comfort that is acceptable. These two aspects should be considered thoroughly and simultaneously.

The aim of stratified ventilation systems is to properly ventilate the occupied zone of the room and leave the other areas more or less unventilated. As a result, the airflow rate and energy use will be reduced without reducing the venting of the occupant area. However, selecting stratified ventilation in a room will set other requirements on the evaluation of a number of other parameters to be compared with those from the traditional method of mixing ventilation, such as location of persons in the room, inlet temperatures and location of devices.

This dissertation will highlight some of the strengths and limitations that are associated with the stratified ventilation system.

1.3 Aim

The aim of this thesis is to contribute to the knowledge and understanding of how different supply devices based on stratified ventilation system work and which parameters have an influence on their performance.

The overarching aim with this project is to analyze and compare different supply devices based on stratified ventilation, with different setups, related to thermal indoor climate, energy efficiency and ventilation efficiency. The analysis is performed using experimental

and numerical investigations. The measurements have been carried out in well-insulated full-scale test rooms in a laboratory hall at the University of Gävle. The simulation of the temperature and velocity distribution in the room are performed by solving the governing equations for the conservation of mass, momentum, energy and the radiative heat exchange between the surfaces by using a commercial CFD code.

1.4 Research questions

This thesis will focus mainly on three research questions:

1. Interaction between a supply device based on stratified ventilation and windows.
2. Flow behavior, energy performance and air change effectiveness for different supply devices based on stratified ventilation.
3. Thermal comfort for different supply devices based on stratified ventilation.

1.5 Limitations

The limitations in this dissertation are summarized below. First, the work has focused on office environments and only a few setups were used to study the influencing parameters. No measurements have been made in real environments where a more dynamic environment applies; all experiments have taken place in steady-state cases. This applies to both simulations and measurements.

Other restrictions include access to measurement points in the experiments performed: measuring temperatures, air exchange and speeds at a few points in the room provides limited information. In some articles, simulations to get a more complete picture of the room have compensated for this weakness. Measurement of velocity has been carried out by hot-wire and hot-sphere anemometers, which involve high uncertainties when measuring flows with high turbulence or low velocities. The CFD study considered steady-state cases and eddy-viscosity turbulence models have been used, due to affordable computational sources, reasonable accuracy and complex geometries of the studied cases.

1.6 Research plan

Research question 1 (see section 1.4) is treated in Papers I and II, see Table 1. Paper I explores experimentally and numerically the thermal performance of a well-insulated window and reveals those parameters that are important for minimizing heat transport through the fenestration. Paper II investigates numerically the interaction between a well-insulated window in an office space ventilated by a stratified ventilation system.

Research question 2 is treated in Papers III, IV, V, VI and VII, see Table 1. Paper III is a numerical comparison of the ventilation performance of different air supply devices in an office environment, where the office room is a single or double occupant room. Paper IV is an experimental study of three different ventilation systems in an open plan office. Paper V is an experimental comparison of ventilation performance of three different air supply devices in a single office room. Paper VI analyzes the air change efficiency in a single office room; the room is ventilated by impinging jet ventilation. Paper VII is an experimental comparison of thermal comfort and ventilation effectiveness for three different air supply devices in a single room

Research question 3 is treated in Papers III, IV, and VII, see Table 1.

Table 1. Articles linking to the research questions.

RQ/Paper	I	II	III	IV	V	VI	VII
1	×	×					
2			×	×	×	×	×
3			×	×			×

1.7 Research method

Two methods have mainly been used in this thesis, measurements and CFD (Computational Fluid Dynamics) simulations. Measurements have been carried out in all of the papers, but two of the papers refer only to measurements from previous articles. For the rest of the papers measurements are reported. CFD is used in four of the papers.

For numerical experiments the CFD code ANSYS and FIDAP have been used. CFD using the Reynolds Averaged Navier-Stokes equations is employed for turbulence modelling.

Measurements have been performed with thermocouples, Hot-Wire Anemometry (HWA) and Hot-Sphere Anemometry, thermal comfort measurement equipment and tracer gas measurement equipment.

The measurements have been used for validation of the numerical models and for experimental analyses of different setups. The numerical simulations have also been used for parametric studies.

1.8 Appended papers

Paper I

Larsson, U., Moshfegh, B. and Sandberg, M. (1999). Thermal analysis of super insulated windows (numerical and experimental investigations). *Energy and Buildings*, 29, pp. 121-128.

In this paper the thermal performance of a well-insulated window has been investigated both numerically and experimentally in a full-scale test room. The window under consideration is a low-emissive triple glazing window with two closed spaces filled with the inert gas krypton. An oxidized metal with low emissivity factor coats one pane in each space.

Experimental and numerical investigations on the thermal performance of the window have been conducted for different winter cases. Temperature data obtained by direct temperature measurement using thermocouples and through numerical analysis are presented. The heat transfer through a window construction depends on three mechanisms, i.e., conduction, convection and radiation. In this paper the convection-conducting mechanisms have been closely investigated. The numerical predictions agree well with the results from the measurements.

Paper II

Larsson, U. and Moshfegh, B. (2002). Experimental investigation of downdraft from well-insulated windows. *Building and Environment*, 37*,* pp. 1073-1082.

The intention of this paper was to investigate the downdraft below a well-insulated window. Measurements of the velocity and temperature in the area close to the window were performed. The experimental setup, of interest here, was for a well-insulated triple-glazed window and a conventional triple-glazed window. The windows were mounted in different positions inside the wall, to create different widths of the window bay. In addition, cases with different supply airflow were investigated.

The experiments were carried out in a well-insulated test room with the window mounted in a wall, with one side against the test room and the other against a cold room. Therefore, outside temperatures down to -20ºC were simulated on one side of the window. To create different widths of the window bay, the window is moved inside the wall. The width of the window bay is varied from 0 to 140 mm. Also, one case with a conventional triple-glazed window was carried out as a reference case. The ventilation of the room was executed by displacement ventilation. The supply airflow in all cases was 0.01 m^3/s except one where the flow was 0.015 m^3/s. Velocities and temperatures were measured in a steady-state condition. The temperature was measured with copper-constantan thermocouples; the temperature measured was the room air temperature, the temperature close to the wall below the window and also the surface temperature at the window pane and at the surrounding walls. The velocity was measured with Hot-Wire Anemometry of the Constant-Temperature type; only the velocity close to the wall below the window was measured.

Paper III

Chen, H. J., Janbakhsh, S., Larsson, U. and Moshfegh, B. (2015). Numerical investigation of ventilation performance of different air supply devices in an office environment. *Building and Environment*, 90*,* pp. 37-50.

This paper compared ventilation performance of four different air supply devices in an office environment with respect to thermal comfort, ventilation efficiency and energy-saving potential, by performing numerical simulations. The devices have the acronyms mixing supply device (MSD), wall confluent jets supply device (WCJSD), impinging jet supply device (IJSD) and displacement supply device (DSD). Comparisons were made under identical setup conditions, as well as at the same occupied zone temperature of about 24.2ºC achieved by adding different heat loads and using different airflow rates. Energy-saving potential was addressed based on the airflow rate and the related fan power required for obtaining a similar occupied zone temperature for each device.

Results showed that the WCJSD and IJSD could provide an acceptable thermal environment while removing excess heat more efficiently than the MSD, as it combined the positive effects of both mixing and stratification principles. This benefit also meant that these devices required less fan power than the MSD for obtaining equivalent occupant zone temperature. The DSD showed superior performance on heat removal, air exchange efficiency and energy saving to all other devices, but it had difficulties in providing acceptable vertical temperature gradient between the ankle and neck levels for a standing person.

Paper IV

Arghand, T., Karimipanah, T., Awbi, H., Cehlin, M., Larsson, U. and Linden, E. (2015). An experimental investigation of the flow and comfort parameters for under-floor, confluent jets and mixing ventilation in an open-plan office. *Building and Environment*, 92*,* pp. 48-60.

There is a new trend to convert workplaces from individual office rooms to open offices with motivation to save money and promote better communication. With such a shift the ability of existing ventilation systems to meet the new requirements is a challenging question for researchers. The available options could have an impact

on workers' health in terms of providing acceptable levels of thermal comfort and indoor air quality. Thus, this experimental investigation focused on the performance of three different air distribution systems in an open-plan office space. The investigated systems were systems with MSD with ceiling-mounted inlets, corner-mounted WCJSD and UFADSD with straight and curved vanes. Although this represents a small part of our more extensive experimental investigation, the results show that all the proposed stratified ventilation systems (WCJVSD and UFADSD) more or less behaved as mixing systems with some tendency for displacement effects. Nevertheless, it is known that mixing systems have a stable flow pattern but have the disadvantage of mixing contaminated air with supplied air, which may produce lower performance, and in worst cases affect occupants' health. For the open-plan office we studied here, it was shown that the new systems are capable of performing better than conventional mixing systems. As expected, the higher air exchange efficiency in combination with lower local mean age of air for corner-mounted WCJSD and UFADSD indicates that these systems are suitable for open-plan offices and are to be favored over conventional mixing systems.

Paper V

Larsson, U. and Moshfegh, B. (2017). Comparison of ventilation performance of three different air supply devices: a measurement study. *International Journal of Ventilation*, 16(3), pp. 244-254.

The aim of this paper was to study the behavior of three different ventilation supply devices, i.e., mixing supply device, displacement supply device and confluent jet supply device, in an office room. The measurements for the present paper were carried out in a special test room at the University of Gävle, Sweden. The room is well-insulated and specially designed for full-scale experiments. The size of the room corresponds to a normal office, to produce a heat load corresponding to an occupied office room with a computer and a person-simulator placed in the middle of the room. The lighting system was working inside the office room during all of the experiments.

Twelve different cases have been studied experimentally with different airflow rates, supply air temperature and supply devices. The results show that the confluent jet ventilation with the device placed at 2.2 m provides the highest value of ventilation efficiency, followed by displacement ventilation, while the lowest ventilation efficiency is found in the mixing ventilation system. The results show small differences in ventilation efficiency between the systems. This can probably be explained by the choice of location of the measuring points. These points were chosen with consideration for a uniform ventilation system such as mixing ventilation. The temperature gradient looks like what one can expect for both mixing and displacement, and confluent jet is a combination of the two. The results also show that the confluent jet ventilation system provides lower air temperature in the occupied zone compared to both displacement and mixing ventilation.

Paper VI

Cehlin, M., Larsson, U. and Chen, H. (2018). Numerical investigation of Air Change Effectiveness in an Office Room with Impinging Jet Ventilation. In Proc. of Cobee 2018 – 4th International Conference on Building Energy and Environment, pp. 641-646.

Providing occupant comfort and health with minimized use of energy is the ultimate purpose of heating, ventilating and air conditioning systems. This paper presents the air-change effectiveness (ACE) within a typical office room using impinging jet ventilation (IJV) in combination with chilled ceiling (CC) under different heat loads ranging from 6.5 – 51 W/m^2. In this study, a validated CFD model based on the v^2-f turbulence model is used for the prediction of airflow pattern and ACE. The interaction effect of chilled ceiling and heat sources results in a complex flow with air circulation. The thermal plumes and air circulation in the room result in a variation of ACE within the room but also close to the occupant. For all studied cases, ACE is above 1.2 close to the occupants indicating that IJV is more energy efficient than mixing ventilation.

Paper VII

Larsson, U. and Moshfegh, B. (2018). Comparison of the thermal comfort and ventilation effectiveness in an office room with three different ventilation supply devices - a measurement study. In Proc. of 14th International Conference of Roomvent & Ventilation, pp. 187-192.

The aim of this paper is to experimentally study the ventilation effectiveness (mean age of air, MAA) and thermal comfort (PMV and PPD) of three different ventilation supply devices, i.e., mixing supply device, displacement supply device and wall confluent jet supply device, in an office room.

The measurements for the present paper have been carried out in a special test room at the University of Gävle, Sweden. The test room has dimensions of 4.2 × 3.0 × 2.4 m with a volume of 31.24 m^3 (see Figure 1), with the size of the room corresponding to a typical office. To produce a heat load corresponding to an occupied office room, one person-simulator was placed in the middle in the room. To produce the heat load two switched-on computers were also placed inside. The lighting system was on inside the office room during all the experiments.

The PMV and PPD are comparable to MSD, WCJSD and DSD as it turns out that MSD has poorer comfort than DSD and WCJSD. DSD and WCJSD have more or less the same thermal comfort performance. When comparing the local mean age of air (MAA) for the studied supply devices, the air is significantly much younger for the DSD and WCJSD than for MSD.

1.9 Author's contribution

Paper I, II, V and VII:

These papers were written entirely by the author of this thesis, but Professor Bahram Moshfegh (who is also the author's main supervisor) provided valuable input and important comments on plans and drafts of these papers.

Paper III

The paper was planned and executed by the author of this thesis, Dr. Huijuan Chen and Dr. Setareh Janbakhsh. The authors of the paper were responsible for different ventilation principles, and the author of this thesis was responsible for the displacement ventilation. As far as writing the article is concerned, the introduction and analysis of displaced ventilation in the result and conclusion chapters were done by the author of this thesis. Professor Bahram Moshfegh provided important comments on plans and drafts of this paper.

Paper IV

The author of this thesis was mainly involved in the planning of the measurements and the cases to be measured, the design of the office landscape and the analysis of the results. The measurements were carried out by PhD student Taha Arghand and research engineer Elisabet Linden. Dr. Taghi Karimipanah and Dr. Mathias Cehlin participated in the analysis of the results.

Paper VI

The paper was planned and performed by Dr. Cehlin and the author of the thesis. The numerical setup used in this paper comes from an earlier publication with Dr. Huijuan Chen et al.

2 Indoor environment and air distribution systems

2.1 Distribution system

2.1.1 Mixing Ventilation

Mixed flow distribution is the traditional method for supplying air to buildings. Air is blown in from the ceiling or wall and dilutes the room air in an attempt to provide a uniform temperature and contaminant level through the space. The idea is that the airflow (jet) entering the space at high speed will enter the room in an unoccupied zone. Before it reaches the occupied zone, the jet must be mixed with the room air so that speed has decreased and the temperature has increased to acceptable levels, see Figure 1. If the ventilation efficiency is around 50%, the room can be considered to have good mixing (Etheridge and Sandberg, 1996).

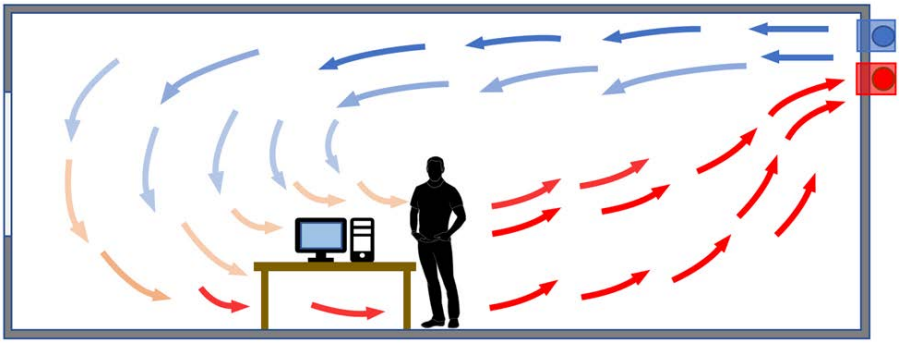

Figure 1. Mixing ventilation in an office.

Mixing ventilation was the first system that was used by engineers to study the significance of indoor ventilation of building and rooms. With developments in recent decades it is now well known that the advantages of this system can be improved upon by other ventilation systems, such as displacement, confluent jet and impinging jet ventilation system (Awbi, 2011).

2.1.2 Stratified ventilation

Stratified ventilation is a concept that often allows good consideration for both indoor air quality and thermal comfort. It uses the buoyancy force by supplying the ventilated room with air colder than the average air temperature in the occupied zone. There is an increase in temperature when the air comes from the inlet device into the room and moves across the floor, see Skistad (1998) and Mundt (1990). Stratified systems are effective in reducing cross contamination, since there is virtually no mixing in the space, the temperature and the pollutant concentration increase linearly from the heat source with the height of the occupied zone, see Skistad (1998) and Mundt (1990).

There are many different ventilation strategies using stratified ventilation systems, such as displacement ventilation, impinging jet ventilation and confluent jet ventilation. Displacement ventilation is a system mainly driven by buoyancy forces. The other two systems, confluent jet and impinging jet, are a hybrid between the mixing ventilation system and displacement ventilation system. They are supposed to meet up for a criterion that displacement ventilation systems are not capable of fulfilling, that the system has a limitations of distance for air to penetrate into the room from the inlet device, see Cao et al. (2014). In this thesis a jet or array of jets that work with walls are considered wall confluent jet and wall impinging jet ventilation.

2.1.2.1 Displacement ventilation

The inlet supply enters the room at a low height close to the floor. Due to buoyancy effects the cold inlet air will fall down to the floor and then spread over the floor until it comes to the heat source. When the flow reaches the heat source the air will be heated and start to rise to the extraction point of the exhaust air located above the occupied zone – preferably close to ceiling, see Figure 2. In the room the air will build up some stratification zones with fresh air and some contaminated air. However, these stratifications can be mixed due to movements in the room, see Sandberg and Mattsson (1992). Displacement ventilation has problems to effectively ventilate areas far from supply diffuser due to its inherent low momentum supply (Awbi,

2008). Displacement ventilation systems do not work for heating a room but could be used for cooling the room.

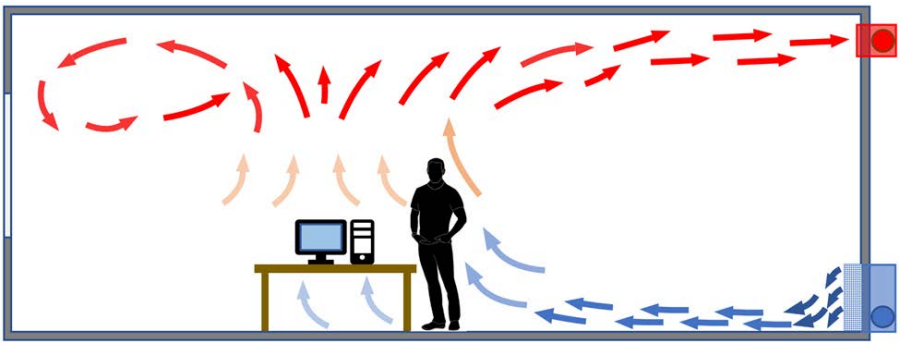

Figure 2. Schematic of displacement ventilation in a room.

Displacement ventilation applications in industrial applications have been around for almost three decades, but are also common in office environments, see Cehlin, Moshfegh and Stymne (2000) and Melikov et al. (2005). However, due to faulty implementation, the system does not function properly. The area close to a displacement device is in many cases located close to the occupants in the room, which can create discomfort for the occupants (Melikov and Nielsen, 1989; Pitchurov et al., 2002). It is also important that the area in front of the system is free, see Figure 3, so the airflow from the device can be developed and create a cross flow into the room.

There have been relatively few comparisons of different setups of ventilation systems during the last three decades, where displacement ventilation has been compared to mixing ventilation systems using different parameters. Nielsen et al. (2005) made an experimental comparison between mixing and displacement in a textile terminal and compared the air distribution, local discomfort and percentage dissatisfied. One earlier comparison was Hu, Chen and Glicksman (1999), who did a computer-simulated comparison of energy use between displacement and mixing ventilation systems in three different U.S. buildings and five climate zones. Karimipanah and Awbi (2002) made a theoretical and experimental investigation of impinging jet ventilation and a comparison with displacement ventilation, but the paper mainly focused on the characteristics of impinging jet

ventilation. Cho, Awbi and Karimipanah (2008) wrote a paper that theoretically and experimentally compared wall confluent jet ventilation with displacement ventilation. Cho, Awbi and Karimipanah (2002) also made a comparison between four different ventilation systems: impinging jet, mixing, wall displacement and floor displacement ventilation systems.

Figure 3. Two bad decisions due to lack of knowledge from the user or HVAC engineer. To the left the system is not working satisfactorily because of blocked items and on the right side a user has stopped the airflow because of discomfort.

2.1.2.2 Impinging jet ventilation

Impinging jet has been used in many industrial applications over the years, for example in electronic cooling (Rundström and Moshfegh, 2006; Larraona et al., 2013), in cooling of metalls (Jahedi and Moshfegh, 2017), cooling of turbine blades (Al Ali and Janajreh, 2015) or drying paper (Mujumdar, 2014). It has also been used in many other industrial applications, with the common parameters for suitable applications in industry as impinging jets offer high rates of heat and mass transfer.

Using impinging jet for ventilating rooms is quite a new strategy. The system was proposed by Karimipanah and Awbi (2002) and later

on by Chen, Moshfegh and Cehlin (2012); Chen, Moshfegh and Cehlin (2013); Ye et al. (2016) and Kobayashi et al. (2017).

The inlet device is quite simple; normally it is the duct that has the role of the supply device. The duct ends at a distance above the floor and the outlet is located close to the ceiling, see Figure 4.

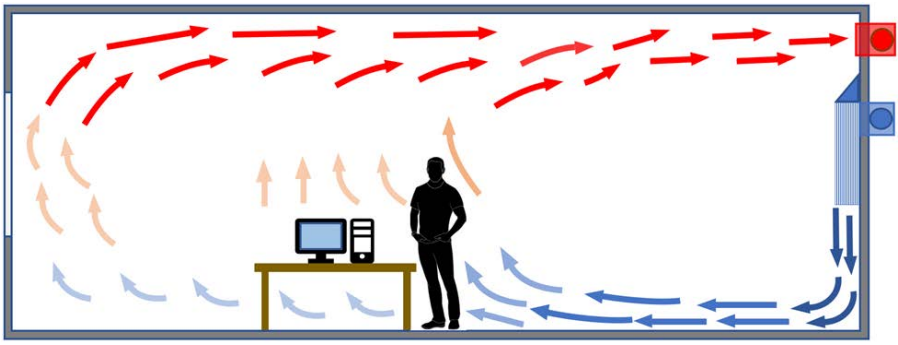

Figure 4. Sketch of the impinging jet ventilation.

The impinging jet with high momentum leaves the supply device and discharges downwards to the floor. After impingement the air will be spread over the floor. A thin layer of air similar to that in displacement ventilation will be created and distribute the fresh air along the floor until it reaches a heat source and creates a rising flow, containing the contaminated air plume, towards the ceiling where it will be extracted by the outlet device.

The risk of the system is that draft occurs in the area near the floor which can be experienced negatively due to the large temperature gradient between foot and head (Melikov, Langkilde and Derbiszewski, 1990); the air can have a relatively high speed and in the case of cooling the temperature may also be low.

2.1.2.3 Wall confluent jet ventilation

The confluent jet system can be defined as a number of free jets supplied in a plane, parallel to each other. Near the diffuser, the confluent jets behave as separate jets, but downstream the jets start to merge with each other and finally behave as a single jet (Awbi, 2003),

see Figure 5. Numerical simulations and measurements by Ghahremanian and Moshfegh (2014) showed that after a certain distance from the device the confluent jets have merged into one jet and the single jets can no longer be recognized.

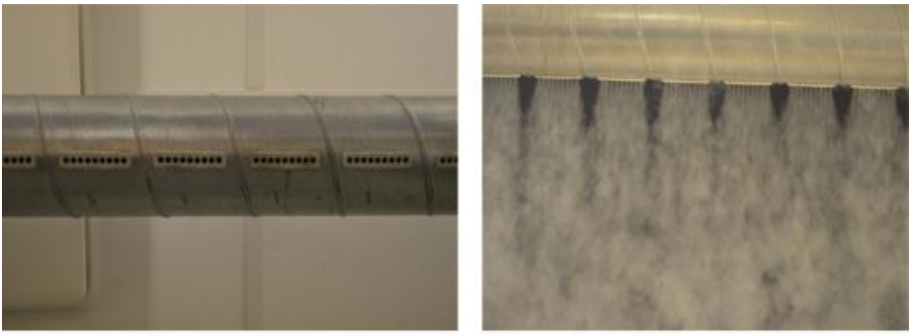

Figure 5. a) Confluent nozzles installed on a ventilation pipe to make the air jet diffuser and b) smoke visualization of the system in operation (Kabanshi, Wigö and Sandberg, 2016).

The supply device is a duct with circular nozzles with a certain number of rows that are located at a certain distance above the floor. The jets are supplied with high relative velocity compared to airflow from displacement devices, which is also the reason for using confluent jets for ventilation in building applications. With a higher velocity (momentum) of the air from the device the air can have a deeper penetration into the room than airflows from displacement ventilation devices. Therefore, this system could be suitable for both cooling and heating. Confluent jet can be considered high momentum supply devices with stratification capability. This method of air distribution combines some positive aspects of both mixing and displacement systems. Despite the high momentum, the velocity decays rapidly after the impingement point on the floor.

Figure 6 below shows a confluent jet of air supplied downward on to the floor with quite a high momentum (i.e., resembling mixing ventilation), but the velocity decays very rapidly away from the point of impact on the floor.

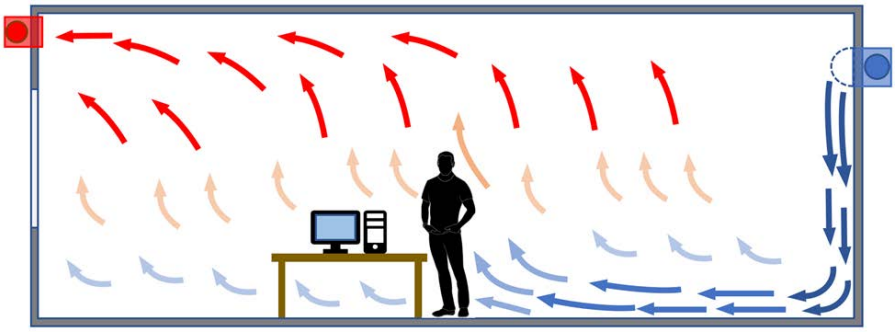

Figure 6. Confluent jet.

The performance of confluent jet systems has been compared with various other systems but mainly with mixing ventilation systems and displacement ventilation systems, both numerically and using measurements. Studies by Cho, Awbi and Karimipanah (2008), Cho, Awbi and Karimipanah (2005) and Janbakhsh and Moshfegh (2014) show that the wall confluent jet creates a greater horizontal spread over the floor than displacement jet. In Karimipanah et al. (2007) parameters such as air quality, comfort and effectiveness for two floor-level air supply systems in classrooms are investigated. The setup for the confluent jet in this paper is confluent jets directed towards the wall in the room corners. For most cases studied in this paper confluent jets performed better than displacement device.

2.2 Temperature gradient

The temperature gradient in a room is an indoor environment comfort parameter to study how the airflow in the room is distributed. The aim of ventilation is to have low concentrations of contaminants and particles and a controlled temperature in the occupied zone.

The buoyancy effects in stratified ventilation are due to the temperature difference between the heated air and the surrounding air. Plumes will be created and a stratification of the air in the room occurs. Stratification generates a temperature gradient along the height of the room.

The aim of mixing ventilation is to mix the air from the inlet with the room air as fast as possible, a total mixing of the air occurs resulting in a homogenous concentration of pollutants and even temperature distribution in the whole room.

Stratification is a way to improve ventilation. For example, with stratification there can be a lower temperature in the occupied zone and a higher temperature in zones above the occupied zone. As a result, a stratified ventilation system can be considered more energy efficient taking into consideration the cooling demand.

2.3 Ventilation efficiency

The ventilation is designed to replace contaminated air with fresh air in a controlled manner, and a number of different air distribution principles can do this. However, just because air is added to a room while removing the same amount of air, there is no guarantee that the desired target is fulfilled, i.e., replacing contaminated air with clean, fresh air. For example, if the air supplied to the room does not pass the occupied zone and goes straight to the exhaust air, we have a classic short circuit of the flow pattern in the room.

To secure good indoor air quality and its performance a number of specific indices describing how efficiently the system achieves these goals have been developed. Etheridge and Sandberg (1996) and Awbi (2003) expressed two, heat removal effectiveness (ε_t) and containment removal effectiveness (ε_c), to characterize the capacity of a ventilation system to remove heat and pollutants from the room. They are expressed in the following equations:

$$\varepsilon_t = \frac{T_o - T_i}{T_m - T_i} \tag{1}$$

$$\varepsilon_c = \frac{C_o - C_i}{C_m - C_i} \tag{2}$$

where C is concentration of pollutants (ppm) and T is the air temperature (°C). *o, i* and *m* represents the outlet, inlet and the mean values in the occupied zone.

The air change efficiency, ε_a, is a measure of how fast the air in the room is replaced in comparison with the theoretically fastest rate, with the same ventilation airflow. The shortest possible air change time for the air in the room, τ_n, which will be obtained in piston flow, is always the same as the local mean age of the air leaving the room. The actual air change time, τ_a, is directly related to the room mean age of air, $\{\overline{\tau}\}$. The actual air change time for all the air in the room, τ_a, is equal to twice the room mean age, $\tau_a = 2\{\overline{\tau}\}$. The air change efficiency, ε_a, is defined as the ratio between the shortest possible air change time for the air in the room, the nominal time constant, τ_n, and the actual air change time, τ_a. Its definition can also be explained as the ratio between the lowest possible mean age of air $\frac{1}{2}\tau_n$, and the room mean age of air $\{\overline{\tau}\}$.

$$\varepsilon_a = \frac{\tau_n}{\overline{\tau_a}} \times 100 = \frac{\tau_n}{2 \times \langle\overline{\tau}\rangle} \times 100\ [\%] \qquad (3)$$

The expected air change efficiency is different for each flow pattern and follows Table 2:

Table 2. Expected air change efficiency for different flow patterns.

Flow pattern	Air change efficiency, ε^a
Ideal piston flow	100%
Displacement flow, confluent jet and impinging jet	$50\% < \varepsilon^a < 100\%$
Fully mixed flow	50%
Short-circuit flow	< 50%

The local air change index, $\varepsilon^a{}_p$, characterizes the conditions at a particular point. It is defined as the ratio between the nominal time constant and the local mean age of air, τ_p, at point p:

$$\varepsilon_p^a = \frac{\tau_n}{\overline{\tau_p}} \times 100\ [\%] \quad (4)$$

In the case of complete mixing the local mean age of air is the same in the whole room and equal to the nominal time constant, this giving a local air change index equal to 100% in the whole room.

2.4 Thermal Comfort

The thermal indoor climate is a complicated combination of a number of physical variables, all of which strongly affect people's well-being. The indoor climate not only has a vital effect on people's health and life quality, but also their productivity and ability to work efficiently. The basis for people to feel a good thermal comfort is to have some neutral heat exchange with the surroundings, i.e., heat losses from the body are on the same level as the body's production of heat to keep a body temperature of 37°C. The heat exchange between the body and the surroundings occurs by conduction, convection, radiation or/and vaporization.

In indoor environments it is not so common that heat exchange by conduction creates any major discomfort, only if one has bare feet on cold floors. Heat losses by convection are more common because forced air movements, e.g. from ventilation systems, against the body increase the heat losses, but natural convection due to the temperature difference between the body and the surrounding air also increases the loss. Cold or warm surfaces, relative to the body temperature, create exchange of heat by radiation. The warm and cold surfaces can be related to heating systems, cooling systems and/or to building parts. The fourth way of heat exchange of the body with the surroundings is by vaporization or condensation of water vapor on the body. For example, perspiration is one way for the body to get rid of heat to the surroundings.

There are several parameters that have an influence on the thermal neutrality of a whole body. The parameters can be divided into two categories: parameters depending on the person or on the environment.

- Air velocity

- Air temperature
- Radiant temperature
- Relative air humidity
- Activity level (met)
- Thermal insulation of clothing (clo)

Air velocity and air temperature are the vital parameters that have effect on heat exchange due to convection. The difference between surface temperature of the body and the surrounding surfaces is the source for the radiation heat exchange. By increasing the relative humidity of the air, the heat losses from the body due to vaporization will decrease. If the relative air humidity reaches 100%, the heat losses from the body by perspiration will decrease to zero.

Models that describe relations between the thermal environment and the psychological health parameters of people who are exposed to an indoor climate have been investigated by several researchers. Fanger (1967; 1970) conducted a heat balance approach between the human body and the environment for comfort analysis:

$$K = H - E_d - E_{sw} - E_{re} - L \tag{5}$$

$$K = R + C \tag{6}$$

where:

K = heat transfer from the skin to the outer surface of the clothed body [W]
R = heat losses from the clothed body by radiation [W]
C = heat losses from the clothed body by convection [W]
H = internal heat production in the human body [W]
E_d = heat losses by water vapor diffusion through skin [W]
E_{sw} = heat losses by perspiration from the skin [W]
E_{re} = heat losses by latent respiration [W]
L = heat losses by dry respiration [W]

These terms are formulated as a steady state equation and the human thermoregulatory system is able to establish this balance within some limits. The temperature, T_s, of the skin is obtained in the formulation of K and E_d. The skin temperature and perspiration are the parameters

that have an effect on heat balance due to the activity level. Fanger (1970) did climate chamber experiments for the purpose of finding relations between skin temperature and perspiration due to activity level, clothing insulation and environmental conditions. The thermal influence of activity, clothing and environmental parameters on the perception of the thermal indoor climate have been closely investigated since the early 1970s (Fanger, 1967; Fanger, 1970; Fanger, Højbjerre and Thomsen, 1974; Fanger, 1977; Fanger et al., 1988).

Three commonly used thermal comfort models are PMV (Predicted Mean Vote), PPD (Predicted Percentage Dissatisfied) and DR (Predicted Percentage of Dissatisfied due to Draft), all derived from Fanger's studies.

The PMV model combines four physical variables (air temperature, air velocity, mean radiant temperature and relative humidity) with two personal parameters: clothing insulation and activity level. Fanger (1970) correlated the thermal load to the PMV index. The PMV model is designed for a large group of people and therefore the index should also consider the deviation from the average. The PMV index reveals the thermal sensation with a scale from +3 to -3, see Table 3. The PMV index is mathematically complex to compute so Fanger (1970) created some look-up tables, and these tables and graphs are also provided in modern comfort standards, e.g. International Organization for Standardization (2005). In ISO 7730 you can also find a programming code to use for the calculation of the PMV index. However, the PMV equation can be written as:

$$PMV = (0.303 \cdot e^{-0.036 \cdot M} + 0.028) \cdot L \tag{7}$$

where:

$L = L(M, l_{cl}, T_{mr}, v_a, T_a, w)$
M = metabolic rate
l_{cl} = thermal resistance of clothing
T_{mr} = mean radiant temperature
v_a = relative air velocity
T_a = air temperature
w = moisture content

Table 3. Thermal Sensation Scale.

+3	+2	+1	0	-1	-2	-3
Hot	Warm	Slightly warm	Neutral	Slightly cool	Cool	Cold

Taking into consideration that the PMV index is intended for a large group of people, Fanger also derived a second index which quantifies the percentage of dissatisfied persons with the indoor climate. This index is called PPD (Predicted Percentage of Dissatisfied) and it is a function of PMV:

$$PPD = 100 - 95 \cdot e^{-(0.03353 PMV^4 + 0.2179 PMV^2)} \quad (8)$$

The PMV index is related to the comfort for the whole body, for example when one part of the body is cold and another is warm the thermal load from the body can be zero and the PMV = 0. The experience of the thermal comfort will of course be influenced if one part of the body is cold. McIntyre (1979) and Fanger et al. (1988) established a new index called DR index that takes into consideration the local discomfort. The DR index is called Fanger's draft model. Draft is defined as *"*an unwanted cooling of the human body caused by air movement.*"* The DR index is a function of local climate parameters, such as air temperature, T_a, average velocity of the air, v_a, and the turbulence of the air, T_u and predicts the percentage of dissatisfied due to draft. Thus,

$$DR = (3.14 + 0.37 \cdot v_a \cdot T_u)(34 - T_a)(v_a - 0.05)^{0.62} \quad (9)$$

For $v_a < 0.05$ m/s use $v_a = 0.05$ m/s

For $DR > 100\%$ use $DR = 100\%$

3 Methods

Numerical simulations and experimental methods are often used to study distribution of temperature, velocity and contaminants in the indoor environment. Thermal comfort studies and ventilation effectiveness are also performed with these two methods.

To analyze the different setups included in this thesis, measurements of a number of parameters have been performed as well as computer simulations (CFD). Measurements are used for the purpose of obtaining data to analyze the function of the different cases that have been handled, but they have also been partially implemented for the purpose of validating the numerical models solved using computer simulation tools. CFD provides more information about indoor environments than measurements, which are normally taken at relatively few points in the room.

3.1 Measurements

The purpose of measuring is to get data to analyze the indoor climate. Measurements in the case of indoor climate are divided into two categories, point-measuring method and whole-field measurements method. The weakness in point-measuring methods is the limitation of points in the room that it is practical to measure, but these are normally easy and fast to do and in many cases provide enough information. The whole-field measurements provide a lot of information over a large area or volume simultaneously.

Temperatures such as surface temperatures, air temperatures and operating temperatures are measured. Velocities, thermal comfort and ventilation effectiveness are also measured.

3.1.1 Velocity measurement

Hot-wire anemometry (HWA) is a measurement technique used to measure gas velocities, in this case air. It works so that the air, with a certain velocity flowing over a heated wire sensor or probe, is at a constant temperature, and loss of energy occurs due to convection. By measuring the feedback from the probe which is connected to an

electric circuit, the loss of energy from the probe wire with constant temperature can be obtained. This relates to the speed of air flow across the wire.

The single-sensor probe is used here to measure velocities in a one-dimensional flow with no changes in the flow direction. The single-sensor wire-probe type 55P81 by Dantec Measurement Technology has been used. The probe is calibrated with the Dantec calibration system.

The digital measurement system, see Figure 7, consists of an anemometer, low-pass filter, signal-conditioning unit, A/D converter and a computer. The signal-conditioning unit has a CTA unit module that keeps the probe at a constant temperature of 220ºC. The output voltage from the hot-wire anemometer passes through the low-pass filter where the high-frequency noise is eliminated after the low-pass filter and the signal will be transferred to the signal conditioning unit. The signal-conditioning unit will adjust the signal to the voltage range of the A/D converter. Inside the computer the signal is transferred into velocities due to the probe calibration, see Bruun (1995).

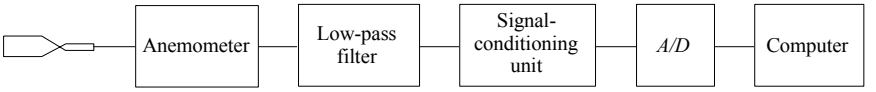

Figure 7. The digital measurement system.

During the calibration, the probe is located in a similar way as in the real case in order to reduce the overheating-induced convection around the probe. Several closer investigations have been carried out for the necessity of correct calibration. These investigations show that the measurements are sometimes not reliable, if the velocity is too low. In some cases, the lowest reliable velocity is 10 – 15 mm/s, see Cowell and Heikel (1988). However, there investigation was performed under circumstances uncommon in a practical case, where the flow direction and probe orientation is unknown. The lowest reliable velocity in a practical case, according to Paul and Steimle (1977), might be as low as 0.2 m/s.

The calibration equipment used for the measurements here is from Dantec. In Paper II velocities of interest here were from 0.05 – 0.5 m/s. Therefore, the calibration is performed for velocities from 0.05 – 0.5 m/s. The calibration interval was divided into 20 points, on a logarithmic scale. A polynomial curve fit of the order four has been used for these 20 calibrated points. This curve shows a good correlation for the measured points over 0.09 m/s (less than 2%). For velocities between 0.05 and 0.09 m/s the deviance from the curve is much higher (up to 10%).

3.1.2 Temperature measurements with thermocouples

Using thermocouples for temperature measurement is a typical point-measuring method. Thermocouples of type T are used for the temperature measurements. Type T consists of copper-constantan and has, according to the manufacturer, a maximum accuracy of 0.5ºC in the range from 0ºC to +133ºC. However, for the present study with temperatures around +20ºC, this type of thermocouple shows an accuracy of 0.2ºC. A PC-based program called Dalite is generally used, but to collect the signals from all the thermocouples and for the conversion from voltage to degrees, Datascan data logger was used. The program stores all the temperature data in files.

The temperatures measured in this study are both the air and surface temperatures. There is a problem with thermocouple wires when a surface temperature is to be measured, because if the thermocouple wire crosses the boundary layer, there will be a conduction heat transfer between the air and the thermocouple. To eliminate this problem, the thermocouple wires have been positioned in an isothermal condition. For the cases with big difference between the surface temperature and the surroundings, the thermocouple has been covered by a thin plate with glossy aluminum tape with low emissivity to minimize the heat exchange due to radiation.

3.1.3 Temperature measurements with infrared camera

Using infrared camera as measurement equipment is a typical whole-field method. The technique of using an infrared camera is to record temperatures over a surface with infrared detectors to generate

thermal images corresponding to the surface temperature. To visualize the flow pattern and temperature distribution around air inlets, thermal images were recorded using an infrared camera S60 (FLIR System). The temperature accuracy was approximately ±2% or ±2°C of reading in the range of -10°C to +55°C.

3.1.4 Tracer gas

Measuring the ventilation efficiency was done by a tracer gas analysis following the decay method (Etheridge and Sandberg, 1996), where tracer gas is injected into a room and mixed with the room air to a uniform concentration. Injecting the gas in the jet from a mixing fan is often necessary. In smaller rooms, one mixing fan is sufficient, but in larger spaces several fans may be required. For the analysis of the tracer gas part, the equipment used is the Multipoint Sampler and Doser: Brüel & Kjaer Type 1303.

In the realization of this experiment, N_2O is the tracer gas selected. Formerly, dinitrogen oxide was widely used for ventilation efficiency in buildings, primarily in Europe. In the US it was rarely used because of its TLV (threshold limit value) of 50 ppm.

In previous tracer gas analysis, SF_6 was the most common gas. Nevertheless, in some countries of the European Union like the United Kingdom it has been prohibited in recent years because of its hazardousness. Sweden is close to following this prohibition. For this reason, N_2O is used during this analysis, since it is safer for people who use it. The N_2O gas is not naturally present in room air in high concentration, hence it would influence the measured concentration.

3.1.5 Thermal comfort

For the analysis of the thermal comfort part, four devices called transducers are used. The first transducer measures air temperature and is shielded against thermal radiation to ensure that the actual air temperature is measured. The second is an air humidity transducer that measures the dew point temperature. The third is an air velocity transducer that measures the air velocity in the indoor environment. The fourth transducer simulates the human body by measuring the operative temperature. All four are necessary input for the thermal

comfort evaluation. The accuracy for the transducers is ±0.2°C for temperatures and ±5% for the humidity and velocity measurements. Operative temperature and thermal comfort evaluation ±0.3°C in the range of 5 – 40°C.

The transducers are connected to a data logger (INNOVA 1221) to collect data and analyze the thermal comfort results according to ISO 7730/CEN 27730. Several research studies have used this equipment to perform thermal comfort measurements, for example see Liu, Rohdin and Moshfegh (2015) and Kabanshi (2016). The following comfort parameters can be calculated by INNOVA 1221:

- Predicted mean vote (PMV)
- Percentage of dissatisfaction (PPD)
- Draft rating
- Turbulence intensity
- Optimal operative temperature
- Equivalent temperature
- Effective temperature
- Required sweat rate
- Wet bulb globe temperature

3.2 Numerical Simulations

Simulating air movements and heat transfer in buildings provides many advantages for gathering the information needed to efficiently design a building´s HVAC systems. Analyzing buildings based on energy and indoor climate can be a very complex physical problem where numerical tools such as Computational Fluid Dynamics (CFD) can be very effective. CFD software generates detailed information for the whole domain by using numerical solutions of the partial differential equations governing the flow field, temperature, and concentration.

CFD has been a useful tool for more than 30 years but mostly in industrial applications such as analyzing flows where it is difficult to perform measurements. Examples are high temperature fluids and environments such as nuclear reactors, flood flows, atmospheric flow,

etc. where full-scale measurements cannot be done. CFD is continuously under development in order to cope with larger and more complex geometries, higher resolution, but also new and more developed physical models and efficient numerical methods. The development of CFD can largely be attributed to the powerful development of computer capacities, both in terms of increasing power and decreasing costs.

Nielsen (1974) was one of the first to use CFD to study the indoor environment. Over the years CFD has become an important tool to predict flow field, temperature, and concentration in the indoor environments, e.g. Gan and Awbi (1994), Cehlin and Moshfegh (2010) and Rohdin and Moshfegh (2011). CFD simulations should always be validated against measurements with the intention of ensuring the accuracy of the predicted result.

3.2.1 Governing equations

Navier-Stokes equations are the fundamental governing equations for fluid flow such as the continuity and momentum transport equations. For conservation of energy, inserting another equation into the equation system is also required for the simulation of non-isothermal flows. These are the governing equations for a Newtonian fluid:

Conservation of mass:

$$\frac{\partial \rho}{\partial t} + \frac{\partial (\rho u_i)}{\partial x_i} = 0 \tag{10}$$

Conservation of momentum:

$$\frac{\partial (\rho u_i)}{\partial t} + \frac{\partial (\rho u_j u_i)}{\partial x_j} = -\frac{\partial p}{\partial x_i} + \mu \frac{\partial}{\partial x_j}\left(\frac{\partial u_i}{\partial x_j} + \frac{\partial u_j}{\partial x_i}\right) + S_M \tag{11}$$

Conservation of energy:

$$\frac{\partial(\rho c_p \theta)}{\partial t} + \frac{\partial(\rho u_j c_p \theta)}{\partial x_j} = \frac{\partial}{\partial x_j}\left(k \frac{\partial \theta}{\partial x_j}\right) + S_\theta \tag{12}$$

3.2.2 Turbulence

Flows in fluids are classified as laminar, transitional or turbulent. Flow Reynolds numbers, *Re,* or Grashof numbers, *Gr*, describe in what condition the flow is. Most of the airflows inside a building are turbulent, however in enclosures such as windows, laminar flows are also common. Turbulence can be described as a chaotic flow with random fluctuations within the main flow, with the random fluctuations changing with time. The turbulent flow has a central influence on momentum and heat transfer in the flow and between the flow and its boundaries.

The instantaneous velocity can be written as:

$$u_i = U_i + u_i' \tag{13}$$

where U_i represents the mean velocity and u_i' the fluctuating velocity. This procedure for decomposing the instantaneous motion is referred to as the Reynolds decomposition. The mean velocity can be stated by ensemble-averaging, thus:

$$U_i = \frac{1}{N} \sum_{n=1}^{N} u_i \tag{14}$$

where N is the number of samples. The variance of the fluctuating part is gained by

$$\overline{u_i'^2} = \frac{1}{N-1}\sum_{n=1}^{N}(u_i - U_i) \tag{15}$$

The turbulent kinetic energy, *k,* can be defined as half of the variations of the three fluctuating velocity components, i.e.:

$$k = \frac{1}{2}\left(\overline{u'^2} + \overline{v'^2} + \overline{w'^2}\right) \tag{16}$$

Furthermore, the turbulent intensity, T_u, is defined by knowing the kinetic energy and a reference mean flow velocity, U_{ref}, as:

$$T_u = \frac{\sqrt{\frac{2}{3}k}}{U_{ref}} \tag{17}$$

3.2.3 Time-averaged transport equations

The time-dependent Navier-Stokes equations of fully turbulent flows need extremely massive computing power to be solved, considering the wide range of length scales and frequencies that occur in turbulent flows. However, the independent variable, e.g. u_i, can be defined as the sum of a steady mean component U_i and a time-varying fluctuation component u_i' with zero mean value. This approach is known as the Reynolds decomposition and the resulting time-averaged Navier-Stokes equations are called Reynolds-averaged Navier-Stokes equations (RANS). Solution of the RANS equations and the averaged heat transport equation provides information on the time-averaged properties of the flow, e.g. mean velocities, mean pressure, mean stresses, and mean temperature. The time-averaged, steady-state, incompressible governing equations can be written as:

$$\frac{\partial(U_i)}{\partial x_i} = 0 \tag{18}$$

$$\frac{\partial(U_i U_j)}{\partial x_j} = -\frac{1}{\rho}\frac{\partial P}{\partial x_i} + \upsilon\frac{\partial}{\partial x_j}\left(\frac{\partial U_i}{\partial x_j} + \frac{\partial U_j}{\partial x_i}\right) + \frac{\partial}{\partial x_j}\left(-\overline{u_i' u_j'}\right) + \beta(\Theta_0 - \Theta)g_i \tag{19}$$

$$\frac{\partial(\Theta U_j)}{\partial x_j} = \alpha\frac{\partial^2\Theta}{\partial x_j \partial x_j} + \frac{\partial}{\partial x_j}\left(-\overline{u_i'\theta'}\right) \tag{20}$$

The equations above encompass additional unknowns, i.e., the Reynolds stresses, $-\overline{u_i' u_j'}$, and the turbulent heat fluxes, $-\overline{u_i'\theta'}$. The Reynolds stresses and the turbulent heat fluxes must be modeled to solve the equation system. It is the core task of turbulence modeling to develop models of satisfactory accuracy and generality to forecast the Reynolds stresses and the turbulent heat transport terms or other scalar transport terms.

3.2.4 Turbulence modeling

Directly solving Navier-Stokes equations with so-called direct numerical simulation (DNS) requires enormous data capabilities, which is usually not possible in cases handled in this thesis due to limitation in data capacity. To numerically calculate turbulent flows, alternative methods have been developed such as Large Eddy Simulation (LES) and Turbulence Transport Modeling (TTM) models.

3.2.4.1 Direct numerical simulation (DNS)

This method of solving turbulent flows is becoming more common, but solving the entire flow field from large eddies to small eddies requires enormously high computing power. The method works for smaller volumes, but doing so in volumes that exist in the built environment such as office environments that are the main focus of this thesis is not yet possible.

3.2.4.2 Large eddy simulation (LES)

Large eddy simulation (LES) solves the complete time-dependent Navier-Stokes equations for the largest eddies, however the effects of smaller eddies are modeled by a sub-grid scale model. To find out the small eddies in a spatial region, filters are used; examples of filters widely used are the Fourier cutoff filter and Gaussian filter. LES shares some aspects from both DNS and RANS turbulence modelling to solve the turbulent flow in the whole field, which gives quite an accurate solution and at the same time requires an acceptable use of data capacity. Small eddies are more isotropic and are relatively less affected by the macroscopic factors like boundary conditioning than large eddies. Therefore, it is easier to find a model to solve the small eddies than solving the entire volume with a RANS model.

LES has been used in several studies in built environments, see e.g. Zhang and Chen (2000); Knight et al. (2005); Wang and Chen (2010). Though LES still needs a significant amount of computation time, this method is estimated to constantly increase in its application due to the rapid growth of computer capacity and speed.

3.2.4.3 Turbulence transport modeling

The Reynolds-averaged Navier-Stokes equations include the solution of the time-averaged equations, when the turbulent scales of different sizes in the turbulent flow will be modelled. By using the Reynolds-averaged approach the required computation decreases the computer resources greatly, and is widely adopted for practical engineering applications. Eddy viscosity models, which are the most common RANS models, are designed on the assumption that a similarity exists between the action of viscous stresses and Reynolds stresses on the mean turbulent flow. Eddy viscosity models utilize Boussinesq's eddy viscosity hypothesis. According to this hypothesis, the Reynolds stresses can be approximated by:

$$\overline{u'v'} = -\upsilon_t \left(\frac{\partial U_i}{\partial x_j} + \frac{\partial U_j}{\partial x_i} \right) + \frac{2}{3} \delta_{ij} k \qquad (21)$$

The turbulent heat fluxes are modeled by introducing a turbulent thermal diffusivity, which is proportional to the turbulent viscosity. The proportionality constant is called the turbulent Prandtl number, σ_t, i.e.:

$$\overline{u'\theta'} = -\frac{\upsilon_t}{\sigma_t}\frac{\partial \Theta}{\partial x_j} \tag{22}$$

where υ_t is the turbulent eddy viscosity. The turbulent viscosity is not a property of the flow but it describes the characteristics of fluid movement. The eddy viscosity models are divided into three different models but for this thesis only the two-equation eddy viscosity is used. These are defined by the number of differential transport equations that are required for the modeling.

Two-equation models are the simplest models where a solution of two separate transport equations allows the turbulent velocity and length scales to be independently determined. There are several forms of two-equation models. In this thesis the following turbulence models have been used by the author; the v^2-f model and the low Reynolds Stress-omega model. Neither of these models uses any "law of the wall" functions, in order to resolve the sharply varying flow variables in the near-wall regions, there is an excessively large number of cells in the immediate area close to the homogeneous wall. These turbulence models are defined below.

3.2.4.4 The v^2-f model

The v^2-f model is developed on the basis of the Durbin's model (Durbin, 1995) and is similar to the standard k-ε model (Jones and Launder, 1972), but incorporates near-wall turbulence anisotropy and non-local pressure-strain effects. The model consists of four transport equations, i.e., turbulence kinetic energy k, its dissipation rate ε, a velocity variance scale v^2 and an elliptic relaxation function f. The distinct merit of the v^2-f model over the two-equation eddy viscosity turbulence models lies in its use of velocity variance scale v^2 to determine eddy viscosity, μ_t, rather than the turbulence kinetic energy k. The v^2-f model is a general low Reynolds number turbulence model

that is valid all the way to the solid wall, and therefore no wall function is required (Fluent, 2010). In the v^2-f model, eddy viscosity μ_t is determined by:

$$\mu_t = \rho C_\mu v^2 T \tag{23}$$

where v^2 is the wall normal stress component, T is the turbulent time scale. k, ε, v^2 and the elliptic relaxation factor, f, are obtained from the following equations:

$$\frac{\partial}{\partial x_j}\left(\rho U_j k\right) = \frac{\partial}{\partial x_j}\left[\left(\mu + \frac{\mu_t}{\sigma_k}\right)\frac{\partial k}{\partial x_j}\right] + \mu_t\left(\frac{\partial U_i}{\partial x_j} + \frac{\partial U_j}{\partial x_i}\right)\frac{\partial U_i}{\partial x_j} - \rho\varepsilon \tag{24}$$

$$\frac{\partial}{\partial x_j}\left(\rho U_j \varepsilon\right) = \frac{\partial}{\partial x_j}\left[\left(\mu + \frac{\mu_t}{\sigma_\varepsilon}\right)\frac{\partial \varepsilon}{\partial x_j}\right] + C_{\varepsilon 1}^{*}\frac{1}{T}\mu_t\left(\frac{\partial U_i}{\partial x_j} + \frac{\partial U_j}{\partial x_i}\right)\frac{\partial U_i}{\partial x_j} - C_{\varepsilon 2}\rho\frac{\varepsilon}{T} \tag{25}$$

$$\frac{\partial}{\partial x_j}\left(\rho U_j v^2\right) = \frac{\partial}{\partial x_j}\left[\left(\mu + \frac{\mu_t}{\sigma_k}\right)\frac{\partial v^2}{\partial x_j}\right] + \rho k f - 6\rho v^2\frac{\varepsilon}{k} \tag{26}$$

$$f - L^2\frac{\partial^2 f}{\partial x_i \partial x_i} = \frac{\left(C_1 - 1\right)}{T}\left(\frac{2}{3} - \frac{v^2}{k}\right) + C_2\frac{1}{\rho k}\mu_t\left(\frac{\partial U_i}{\partial x_j} + \frac{\partial U_j}{\partial x_i}\right)\frac{\partial U_i}{\partial x_j} + \frac{5}{T}\frac{v^2}{k} \tag{27}$$

$$\text{where } C_{\varepsilon 1}^{*} = C_{\varepsilon 1}\left(1 + 0.045\sqrt{\frac{k}{v^2}}\right) \tag{28}$$

The turbulent time scale T and length scale L are determined by:

$$T = \min\left[\max\left(\frac{k}{\varepsilon}, C_t\left(\frac{\nu}{\varepsilon}\right)^{1/2}\right), \frac{\alpha}{\sqrt{3}}\frac{k^{3/2}}{\nu^2 C_\mu \sqrt{2S_{ij}S_{ij}}}\right] \tag{29}$$

$$L = C_L \max\left[\min\left(\frac{k^{3/2}}{\varepsilon}, \frac{1}{\sqrt{3}}\frac{k^{3/2}}{\nu^2 C_\mu \sqrt{2S_{ij}S_{ij}}}\right), C_\eta\left(\frac{\nu^3}{\varepsilon}\right)^{1/4}\right] \tag{30}$$

The following constants are used in the v^2-f model: C_μ=0.22, σ_k = 1.0, σ_ε = 1.3, $C_{\varepsilon 1}$ = 1.4, $C_{\varepsilon 2}$ = 1.9, C_1 = 1.4, C_2 = 0.3, C_t = 6, α = 0.3, C_L = 0.23, and C_η = 70.

3.2.4.5 The Reynolds Stress-omega Model

The RSM has five more transport equations compared to k-ε models and as a result is more suitable for anisotropic turbulence modelling, such as streamline curvature, swirl, rotation, and rapid changes in strain rate. The RSM model has greater potential to give accurate predictions for complex flows. RSM closes the Reynolds-averaged Navier-Stokes equations by solving transport equations for the Reynolds stresses, together with an equation for the dissipation rate. RSM predictions are still limited by the closure assumptions employed to model various terms in the exact transport equations for the Reynolds stresses.

The first to present this approach were Launder, Reece and Rodi (1975). As in eddy viscosity models, the term turbulent viscosity is used here and is proportional to turbulent viscosity. The RE-stress omega model was set up for the RSM model (Fluent, 2010). The equations for transport of Reynolds stresses can be written as:

$$\frac{\partial \rho \overline{u_i u_j}}{\partial t} + \frac{\partial}{\partial x_k}\left(\rho U_k \overline{u_i u_j}\right) = P_{ij} - \frac{2}{3}\beta' \rho \omega k \delta_{ij} + \Phi_{ij} + P_{ij,b} + \frac{\partial}{\partial k_k}\left(\left(\mu + \frac{\mu_t}{\sigma_k}\right)\frac{\partial \overline{u_i u_j}}{\partial x_k}\right) \tag{31}$$

where P_{ij} is stress production, and $P_{ij,b}$ is the production due to buoyancy. Φ_{ij} is the pressure strain correlation. For more details se (Fluent, 2010).

The transport equation for omega, ω, is given by:

$$\frac{\partial(\rho\omega)}{\partial t} + \frac{\partial(U_k\rho\omega)}{\partial x_k} = \alpha\rho\frac{\omega}{k}P_k + P_{\omega b} - \beta\rho\omega^2 + \frac{\partial}{\partial x_k}\left(\left(\mu + \frac{\mu_t}{\sigma_\omega}\right)\frac{\partial\omega}{\partial x_k}\right) \quad (32)$$

where $\sigma_k = 2$, $\sigma_\omega = 2$, $\beta = 0.072$, $\alpha = 0.52$, P_k is the production term due to stress production and $P_{\omega b}$ is the production term due to buoyancy.

3.2.5 Boundary conditions

To do numerical simulations of a physical model one need to define accurate boundary conditions. The following boundary conditions are used in this study. In Papers III and VI a uniform temperature has been used for the inlet flow. The boundary conditions for velocity for the inlet were provided by measurements or validated CFD simulations. Turbulence intensity was provided by percent at the inlet. Pressure outlet was chosen as the boundary conditions at the outlet. In Paper III and IV zero heat fluxes have been applied from the surroundings except from heat sources. All walls were treated as non-slip conditions with wall function characteristics. For more information, see Paper III and VI.

Paper I simulate fluid flow inside a closed space and have therefore no inlet or outlet conditions. The boundary condition is from measured surface temperatures, analytical calculated heat transfer, and their coefficients. Thermo-physical properties in the closed spaces of the gases and the emissivity of the panes were used for the analytical

calculation. The flow assumed to be two-dimensional and laminar and the surfaces grey-diffused. For more information, see Paper I.

3.2.6 Mesh strategies

Performing reliable results from CFD simulations requires a large number of cells in adequate areas in the physical model. However, large number of cells generates longer CPU times and therefore has higher demands on the computer resources. Making a good grid design requires knowledge about fluid dynamics.

In Paper III and VI the mesh was generated in AIRPAK. Three-dimensional hexahedral mesh was used. Non-conformal mesh was adapted and placed around the inlet devices and the heat sources. The grid was refined close to solid walls to solve the boundary layers. In Paper I the mesh was generated by FIDAP and a fine mesh was used adjacent to the surfaces in the closed spaces. For more information of the mesh generations, see Paper I, III and VI.

3.2.7 Numerical aspects

The numerical method, discretization schemes, spatial and temporal resolutions, convergence criteria, sampling time, and the solving procedure (e.g. the pressure-velocity coupling) are a number of numerical aspects. These aspects are of considerable importance for both steady and unsteady simulations to ensure the accuracy of the outcome from numerical simulations. Different numerical methods can be used for the discretization, in this thesis; the finite element method (FEM) and finite volume method (FVM) have been used.

In Paper III and VI the finite-volume solver from ANSYS Fluent have been used to numerically solve the governing equations. The FVM was used for discretization. The pressure and velocity coupling was handled with the SIMPLE algorithm. Paper I using a solver from FIDAP to solve the governing equations and the FEM was used for discretization. For more information about the numerical aspects, see Paper I, III and VI.

4 Case Study

4.1 Windows, downdraft and displacement ventilation

Papers I and II in the thesis are mainly about window physics, downdraft and how they interact with displacement ventilation. The method used in Paper I is both numerical calculations and measurements, while in Paper II measurements are used as the method.

The window studied in Paper I is of triple glazed type with three 4-mm panes. The space between the panes is filled with krypton. The oxidized metal on the outside of the inner pane and on the inside of the outer pane reduces the emissivity of the surfaces from about 0.84 to 0.12.

The experimental investigations have been carried out in a special test room at the Department of Built Environment of the Royal Institute of Technology, Gävle, Sweden. The test room has a hot room, a cold room and a guarded room, see Figure 8. In order to provide well-defined boundary conditions the hot room is well insulated. The walls of the hot room are filled with mineral wool of a thickness of about 0.20 m, and the roof and floor are also filled with equally thick mineral wool. The cold room is located next to the hot room. The climate is cold in the Scandinavian countries during the winter and temperatures of -20°C are not unusual. The air temperature in the cold room is stabilized with an on-off controller.

To keep the air temperature level in the hot room at the required level, an electrical heat cable is placed on the floor as a heat source. The heat cable is controlled by a transformer to maintain the right voltage for a certain temperature in the room.

The window under consideration is mounted in the wall between the cold room and the hot room. Temperatures in the cold and hot rooms, as well as surface temperatures of the window, have been measured with copper-constantan thermocouples; about 40 thermocouples were used. The thermocouples used on the pane surfaces have a thin plate mounted and between the plate and the pane a thermal contact paste is applied, see Jonsson (1985). A computer-controlled data acquisition

system was used to evaluate the signals from the thermocouples and then the temperatures were registered and analyzed. Figure 8 shows the configuration of the test room where the measurements have been carried out.

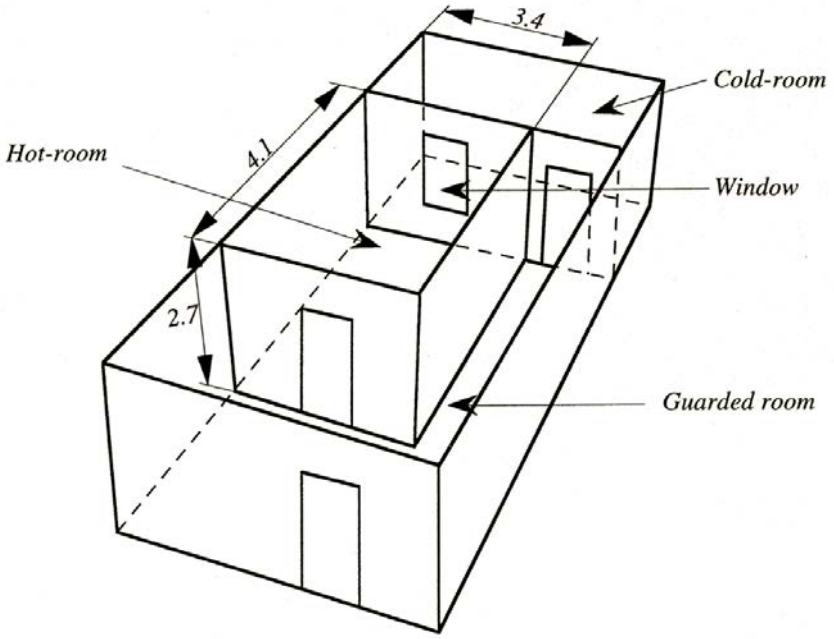

Figure 8. Configuration of the test room (dimensions in m).

The analytical and numerical calculations are analyzed on the glass part of the window, that is, on the window without the frame, see Paper I.

In Paper II the downdraft from windows was under consideration. The intention was to experimentally investigate the downdraft below a well-insulated window and a conventional one. Measurements of the velocity and temperature in the area close to the windows were performed. The experimental setup of interest here is for a well-insulated triple-glazed window and a conventional triple-glazed window. The windows were mounted in different positions inside the wall, to create different widths of the window bay. In addition, cases with different supply air flows were investigated.

The experiments were carried out in the same test room as in Paper I, see Figure 9. The windows were mounted on the outer wall and the dimensions were 1.0 × 1.2 m. The ventilation system in the test room was a displacement ventilation system. The inlet of the ventilation air was located at the back of the room opposite the wall where the window was mounted; see Figure 9. The temperature of the inlet air was about 3 to 4ºC lower than the room air temperature. To compensate for the heat loss through the window and to warm up the ventilation air to the level of room air, an electric resistance mat covered the floor, thus simulating a heated floor.

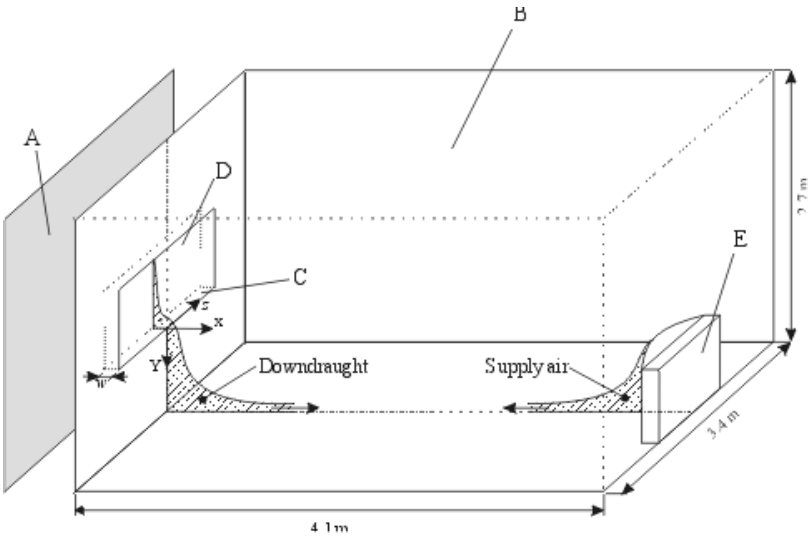

Figure 9. The test room. A) cold room, B) well-insulated room, C) window bay, D) window and E) displacement ventilation device.

For this paper, a well-insulated triple-glazed window (*U*–value is about 1.0 W/m^{2}K) and a conventional triple-glazed window (*U*–value is about 1.8 W/m^{2}K) were used, see Paper II. All measurements are performed with an outside temperature of about –20ºC.

The temperature is measured under steady state conditions; it took about 15 hours for the room to reach steady state conditions after setup. The air temperature was measured at different locations. Test room temperature on the window surface, walls and floor were also measured. In the cold room, the surface temperatures of the window and the air temperature in the middle of the room were measured. Close

to the wall, below the window in the test room, the air temperature was measured in a grid system with 348 measuring points. The thermocouple was moved between the measuring points with a 2–D traversing system. Thermocouples of type T were used for the temperature measurements.

The velocities in the test room were measured under steady state conditions. The velocities of interest here occurred below the window; from 20 mm below the window bay to 120 mm beneath the bay in the *y*–direction (height). In the *x*–direction the velocities were measured from 5 mm to 150 mm from the wall into the test room. In the *z*-direction, the measurements have been taken at two positions, in the mid-plane of the window and for one case the left side of the window at the boundary between the glass and the vertical part of the frame. For the velocity measurements, hot wire anemometry (HWA) with constant temperature (CT) technique was used. The downdraft from a window was assumed to behave as a one-dimensional flow. Thus, a single-sensor probe could be used to measure velocities in a unidirectional flow with no changes in the flow direction wire. The single-sensor wire probe type 55P81 from Dantec Measurement Technology was used. The probe is calibrated for very low velocities, in the range of 0.05 to 0.5 m/s, with the Dantec calibration system.

4.2 Comparison of ventilation systems in office environments

A comparison of performance of different ventilation system setups in office environments is a major part of this thesis. In Papers III, IV, V, VI and VII these comparisons have been made. In Papers III and VI numerical methods have been used, and in Papers IV, V and VII measurements have been the tool used for data collection. The numerical models used in Papers III and VI are validated against measurements but they are not specifically described in these papers.

Paper III considered a comparison of the ventilation performance of four different air supply devices in a small office environment with respect to thermal comfort, ventilation efficiency and energy-saving potential, by performing numerical simulations. The study was undertaken to compare the ventilation performance of the proposed

wall confluent jets and impinging jet supply devices with that of the mixing and displacement supply devices.

In Paper III numerical simulation was used to predict the velocity and temperature in an office environment for four types of air supply devices. Different turbulence models, i.e., the renormalization group (RNG) $k-\varepsilon$ model, shear stress transport (SST) $k-\omega$ model, the $\overline{v^2}-f$ model and the Reynolds stress model (RSM) were employed for the investigation of air supply devices. The chosen turbulence models were verified against experimental results in the previous studies. The RNG $k-\varepsilon$ turbulence model was used successfully for the prediction of the MSD in an office room (Karimipanah, Awbi and Moshfegh, 2008; Cho, Awbi and Karimipanah, 2002). The SST $k-\omega$ model showed a good agreement with the experimental data in the near field of confluent jets (Ghahremanian and Moshfegh, 2014) and in an office room with a wall confluent jets ventilation system (Janbakhsh and Moshfegh, 2014; Janbakhsh and Moshfegh, 2015). For the IJSD, the $\overline{v^2}-f$ model has been validated for both jet region and various zones inside an office environment, see Chen, Moshfegh and Cehlin (2013). For the DSD, the Reynolds Stress Model (RSM) showed the best agreement with the measured temperature and velocity profiles near the DSD, see Cehlin and Moshfegh (2010).

The room under consideration has the dimensions 4.2 m length, 3.6 m width, and 2.5 m height. The mannequin, computer (PC) and lighting were simulated as internal heat loads. The layout of the physical models is shown in Figure 10. The air enters the room through the air supply devices, and room air is extracted at an exhaust outlet placed at the upper corner of the same wall. The MSD is a slot with a length of 0.4 m and a width of 0.02 m, and installed close to the ceiling, i.e., 2.36 m above the floor. In the WCJSD the air issues from the 192 round jets that are placed in an array of 24 × 8. Each nozzle has a diameter of d = 10 mm and spacing center to center between each nozzle in the same row and between two parallel rows is 14 mm. The studied WCJSD is installed at height 1.6 m above the floor. The IJSD is semi-elliptical with an opening area of 0.0166 m^2 and installed at a height 0.8 m above the floor. The DSD is a flat diffuser with the dimensions length by height 0.49 m × 0.4 m, located at 0.09 m above the floor. The devices are installed at the middle of the inlet wall, see Figure 10.

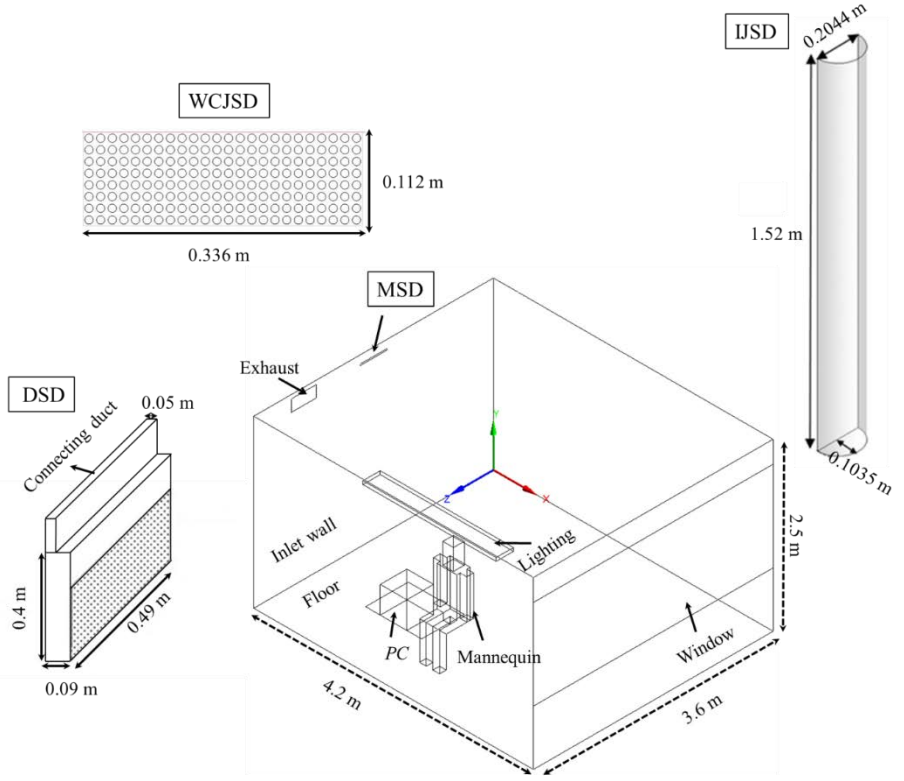

Figure 10. Layout of the physical model.

In Paper IV an experimental investigation of flow pattern and thermal comfort has been investigated for an open plan office with different ventilation supply devices such as under-floor, confluent jet or mixing ventilation devices.

The measurements were carried out in an open-plan office room 8.4 × 7.2 × 2.67 m (i.e., length, width and height) with partitions. The floor and the main ceiling were insulated by 15 cm mineral wool and covered by a layer of plastic sheet to reduce air infiltration. The suspended ceiling consisted of 60 × 60 cm fiberglass tiles located 31 cm below the main ceiling. The room was placed in a large laboratory hall with rather steady temperature condition of 20.7°C ±0.3°C. Since it was supposed to simulate the room's thermal condition for summer, the room was connected to a warm climate chamber where the windows were located. The suspended ceiling was not expected to be thoroughly air

impermeable. The exhaust device was in the middle of the main ceiling. Figures 11 shows the layout of the room. The figure on the left side is a layout of the test room, (*a*) is the electrical foil, (*b*) is the radiators, (*c*) is the light, (*d*) is the wall partition, (*e*) the mannequin and (*f*) is the computer. The figure on the right side shows the configuration of the room and its measurement points: (A) under-floor devices, (B) confluent jet devices, (C) mixing ventilation devices. All dimensions are in meters.

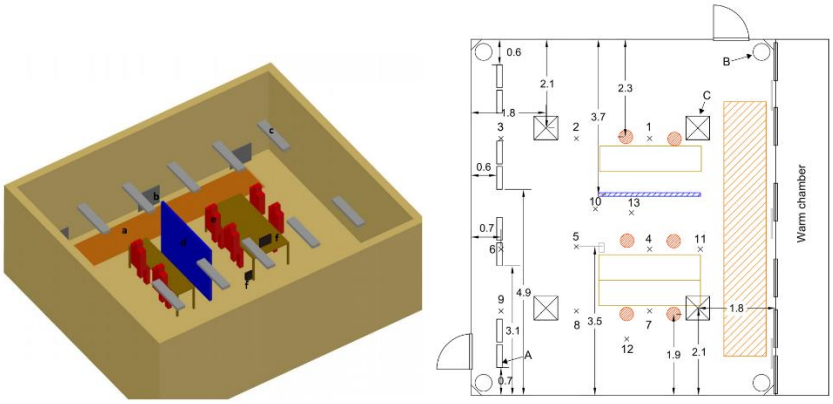

Figure 11 layout of the open plan office.

For velocity and temperature measurements, 27 low-velocity omnidirectional thermistor anemometers located at nine points and three heights (0.1 m, 1.2 m and 1.8 m) were used. The thermistor and the logger system, CTA88, were designed to enable the measurements of low velocities and fluctuations in a room, see Lundström et al. (1990). A plastic shield was used between two sensors to reduce the risk of heating the temperature sensor by the velocity sensor in the case of head-on flow. Therefore, the effect of disturbance could be neglected because of the small dimensions of the equipment. The sampling interval for all measurements was 600 s. The velocity was measured with an accuracy of ±0.05 m/s excluding directional error with a response time of 0.2 s to 90% of a step change. The uncertainty of temperature measurements was ±0.2°C with a response time of 12 s to 90% of the value in still air. It is worth mentioning that all thermistor anemometers had been calibrated before they were used in the room.

Several T-type (copper-constantan) thermocouples were used to measure the vertical temperature gradient in the room and its surrounding temperature as well as supply and exhaust air. The logger and thermocouples were also calibrated afterwards to ensure that the system was performing as expected during the measurements. Therefore, the uncertainty of temperature measurements was estimated to be about ±0.2°C.

Thermal comfort measurements were directly carried out at several measurement points for a seated person at neck level by employing the thermal comfort data logger INNOVA 1221. The logger and transducers were customized for measuring the required physical parameters to evaluate thermal comfort conditions of a room. The time duration for each measurement varied between 50 to 90 minutes depending on the case and the tracer gas measuring time. The sampling time for each parameter was 10 s by using four transducers which were connected to the sockets and set up on the INNOVA 1221 via the RS-232 interface. It is worth mentioning that the PMV calculations were performed using the values of operative temperature, air velocity, humidity and predefined values for clothing and activity level.

Internal heat sources in the room consisted of mannequins, lighting, electrical equipment, aluminum radiators and film heaters which were placed at different locations and heights, see Paper IV.

Papers V and VII were conducted in a test room with dimensions $4.2 \times 3.0 \times 2.4$ m with a volume of 31.24 m^3 (see Figure 12). In these two papers temperature gradient and air exchange efficiency for three different setups of supply devices were measured, i.e., wall confluent jet device, displacement device and a mixing ventilation device.

To produce a heat load corresponding to an occupied office room, one person-simulator was placed in the middle in the room. To produce the heat load two switched-on computers were also placed inside. The lighting system was switched on inside the office room during all the experiments.

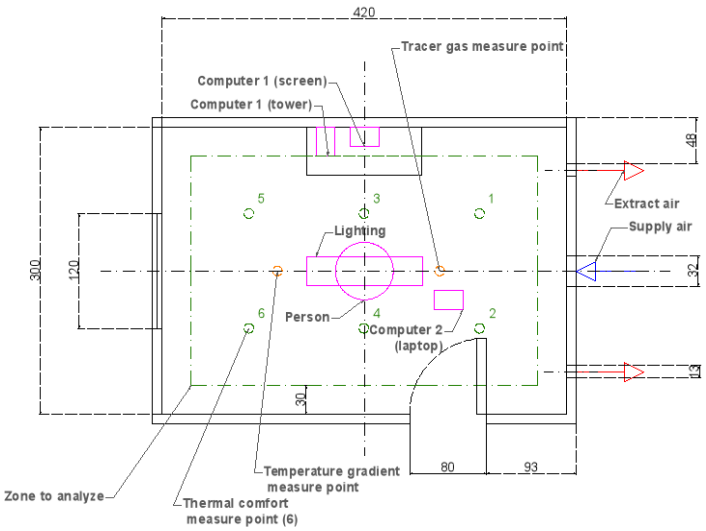

Figure 12. Layout of the office room.

Figure 13 shows the wall where the extract and supply device were mounted. The supply air device shown in the figure is the mixing ventilation system and is located at 2.2 m from the floor. Figure 13 also shows closer pictures of all three devices used in the measurements. The displacement device was located on the floor right below the mixing device shown in the figure and the confluent device was located 2.2 m from the floor or at a height of 1.7 m from the floor.

Measuring the ventilation efficiency was done by a tracer gas analysis following the decay method (Etheridge and Sandberg, 1996) where tracer gas (N_2O) is injected into a room and mixed with the room air to a uniform concentration. Injecting the gas in the jet from a mixing fan is usually necessary. In smaller rooms, one mixing fan is sufficient, but in larger spaces several fans may be required. For the analysis of the tracer gas part, the equipment used is the Multipoint Sampler and Doser: Brüel & Kjaer Type 1303.

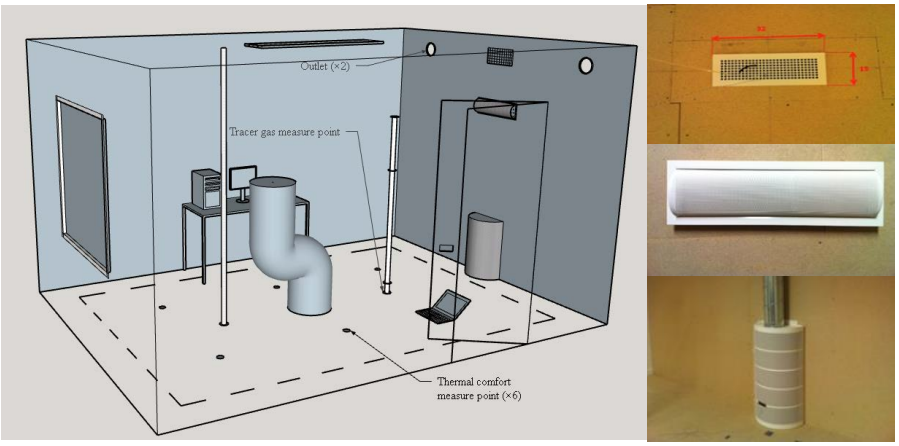

Figure 13. Picture of the room and the devices used in Papers V and VII.

In this case the concentration was measured with five channels: three points were measured at the same location (see Figure 13), but at different heights, 0.1 m, 1.2 m and 1.7 m from the floor. The other two channels measured the concentration in the supply and the exhaust of the ventilation system. The time for the measurement in each case was 12 hr and during the whole measurement the room door was closed. The heights where the concentration was measured were chosen from a reference case, mixing ventilation. Other heights and locations could have been chosen for other systems but it would be more difficult to compare the systems in such case.

For the analysis of the temperature in the office room, the following equipment was used:

- Temperature sensors: They were distributed in a straight line throughout the room at 10 heights, also one in each of the walls, at the supply and exhaust air points, and at the supply and exhaust ceiling points.
- The uncertainty of temperature measurements was ±0.2°C with the response time of 12 s to 90% of value in still air
- Data acquisition switch unit Agilent 34970a

The measurements have been performed for 12 different cases with different airflow rates, supply air temperature and supply device, see Paper V.

The tracer gas measurements were performed to assess the mean age of air and the air change efficiency of the office room.

The aim of Paper VI was to numerically examine the effects, in particular the interaction effects, of chilled ceiling and heat sources on air change effectiveness (ACE) within a ventilated room equipped with impinging jet supply device. Five different cases have been studied by variably cooling the load of chilled ceiling, heat load composition and airflow rate, see Paper VI for more detailed information on the cases considered.

The room with IJSD under consideration had a dimension of 4.2 × 3.6 × 2.5 m, which could be furnished as a single-person or two-person office, see Figure 14. Air was supplied through a duct and discharged at a height of 0.8 m above the floor, and evacuated from the exhaust located below the ceiling at the same side wall. The outlet of the supply device was semi-elliptical with an opening area of 0.0166 m^2; for more information, see Chen, Moshfegh and Cehlin (2012). One rectangular box is used to represent the four lamps installed along the same side of the room. PC and table are attached to the side wall z = 3.6 m, and the ceiling lighting is placed at the position directly above the head.

In a previous publication (Chen, Moshfegh and Cehlin, 2013), a specific numerical setup within the current design space was extensively validated using experimental data for air temperature and air velocities. In the present study, the computational setup was exactly the same as in Chen, Moshfegh and Cehlin (2013). The commercial finite volume code ANSYS Fluent 17.2 was used to numerically solve the governing equations. $\overline{v^2} - f$ model is used as turbulence model. The pressure and velocity coupling is handled with the SIMPLE algorithm. The convection terms were discretized using the second-order upwind scheme, while a second-order central differencing was used for the viscous terms.

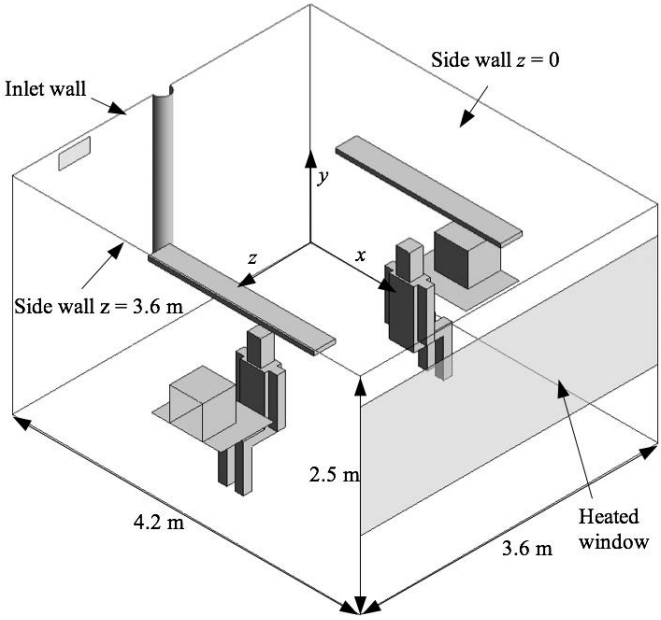

Figure 14. Layout of the physical model used in the case studies.

5 Results

In this chapter some of the results from the appended papers are presented, mainly focusing on these three research questions:

1. Interaction between a supply device based on stratified ventilation and windows.
2. Flow behavior, energy performance and air change effectiveness for different supply devices based on stratified ventilation.
3. Thermal comfort for different supply devices based on stratified ventilation.

Table 4 shows the link between the research question and the related paper. Research question #2 is divided into three different parts.

Table 4. Papers linking to the research questions.

RQ/Paper	I	II	III	IV	V	VI	VII
1	×	×					
2			×	×	×	×	×
3			×	×			×

5.1 Research question #1

Research question #1 focuses on the interaction between a supply device based on stratified ventilation and the windows.

The thermal performance of a window has a major impact on the surface temperature of the inner side of the windowpane. The temperature difference between the windowpane's inner surface and the air temperature in the room can be a source of downdraft. With super-insulated windows the expectation is that in addition to reduced energy loss through the window, there is also improved thermal comfort due to reduced downdraft.

The window used (Paper I) has a very good resistance to heat transmission, *U*–value is 1.0 W/m^{2}K. Over most of the window, for an indoor temperature of 19.0°C and outdoor temperature of –20.6°C, the

temperature on the inner pane is around 15 °C, which represents a difference between room air temperature and temperature on the inner pane of the window of about 4°C. If using a conventional window, *U*–value is 1.8 W/m^{2}K, the velocity of the downdraft is almost 50% higher and the downdraft air has a temperature of 2.2°C lower than that of the downdraft from a well-insulated window.

The relatively high temperatures on the major part of the inner windowpane have a positive outcome which reduces the downdraft. Well-insulated windows enable the use of heating systems other than conventional radiators located below the window, for example floor heating. However, there is still a temperature difference between the room air and the windowpane, which creates downdraft.

An experimental investigation of downdrafts from windows has been performed to study the effect of a displacement supply device on the downdraft (Paper II). Two different setups were performed, a well-insulated window with different supply airflow rates, 10 l/s and 15 l/s.

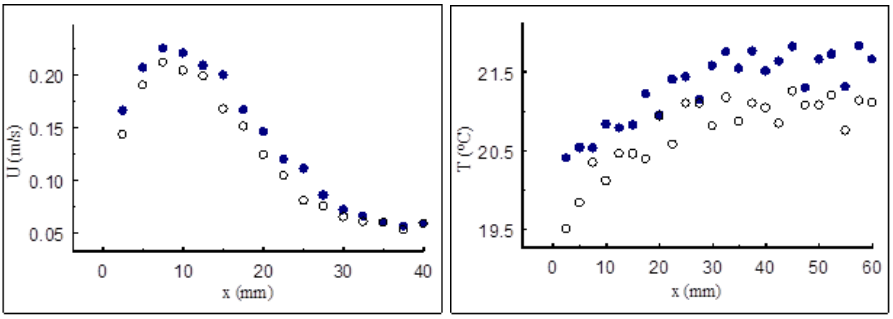

Figure 15. Velocity and temperature profiles for different supply airflows. The solid circle: 10 l/s, and the clear circle: 15 l/s. $U_{max@10\ l/s}$ = 0.23 m/s and $U_{max@15\ l/s}$ = 0.21 m/s. x = distance from the window surface.

In Figure 15 the result of the downdraft was for two different air supplies. The displacement ventilation system used for ventilation of test room was located on the wall opposite to the window. As a result, the air diffuser creates a flow in the opposite direction due to the downdraft. This arrangement of the supply air obviously affects the flow patterns below the window by pushing the air towards the external wall. Thus the magnitude of the supply air from the displacement

diffuser is an important parameter for estimating whether these two systems, i.e., well-insulated windows and displacement ventilation, work in harmony. Normally, in displacement ventilation systems, the velocity from the diffuser is relatively low, approximately 0.2 – 0.3 m/s, at 50 mm from the diffuser. In addition, the distance between the two walls is relatively long, about 4 m and that of course also has an effect on the results.

5.2 Research question #2

Research question #2 focuses on the flow behavior, energy performance and air change effectiveness for different supply devices based on the stratified ventilation.

5.2.1 Flow behavior

Figure 16 below is from Paper III and it shows the flow patterns of four different supply devices: MSD, WCJSD, IJSD and DSD, represented by the iso-velocity = 0.25 m/s together with the corresponding temperature contour plots. These figures were generated using the results for only internal heat sources and the four air-distribution systems were considered. WCJSD, IJSD and DSD generates a much smaller area for iso-velocity = 0.25 m/s, compared to the MSD. The DSD goes more directly into the room than WCJSD and IJSD. DSD also has a lower temperature in the zone close to the device compared to WCJSD and IJSD. The IJSD has more airflow that goes in a perpendicular direction than DSD and WCJSD. Since the air from MSD involved strong mixing between the jet and room air on its way down to the floor, supply air flows were heated rapidly to an appropriate temperature before entering the occupied spaces, i.e., about 23°C. However, the WCJSD, IJSD and DSD directly delivered supply air to the occupied zone. Although the high-level supply devices created more favorable room temperatures for occupants, they might generate higher draft risks due to strong air movements provoked in the room.

The difference in terms of air-flow patterns as well as temperature contour plots between the four air supply systems were essentially related to the characteristics of air supply devices, such as the type and

position, as well as air supply velocities and momentum. In the current configuration of MSD, the position of heat sources (i.e., occupant, etc.) played a role in determining the room air-flow pattern, because buoyancy from the heat sources tended to force the flow attached to the ceiling towards the other side of the room. As a result, the supply air-flow seemed to be directed towards one corner of the room and consequently covered a large area near the floor, as shown in Figure 16.

In the WCJSD, the wall confluent jets remained attached to the wall due to the Coanda effect and moved downward towards the floor. The jet across the floor is attached to the floor boundary away from the stagnation zone. In the IJSD, the air flow was supplied with a high momentum, at a certain height above the floor, which was lower than that for the MSD and then distributed radially after impingement. Although high momentum was supplied by WCJSD and IJSD systems, the velocities near the floor (e.g. at the level of 0.1 m) were reduced to an acceptable level but still sufficient for providing effective air distribution. Entrainment in the case of WCJSD and IJSD are less than for systems with MSD. In the case of the DSD, the air was supplied from a wall-mounted plane diffuser with a low momentum and discharged forwards to the room. The air-flow pattern behaved somewhat like a two-dimensional flow and provides the lowest temperature between the jet and room air in comparison with the four air supply devices studied.

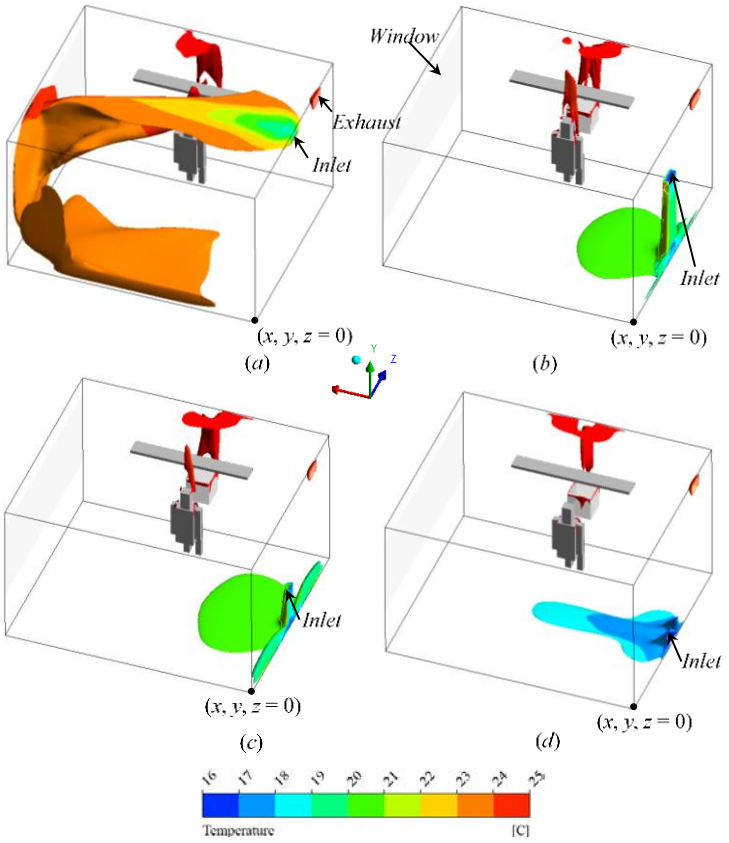

Figure 16. Iso-surface of the velocity for 0.25 m/s together with its corresponding temperature contour plots for (a) MSD, (b) WCJSD, (c) IJSD and (d) DSD.

Vertical temperature distribution in the mid-plane of the room for all four supply devices is shown in Figure 17. The results are for the case of internal heat loads only. It could be seen that the MSD provided quite uniform thermal conditions in the room with a temperature of about 24.5°C. As the mixing effect was reduced while thermal stratification was enhanced for other systems, the vertical temperature difference increased and, as a result, a lower room air temperature was provided. This could be noted for the WCJSD and IJSD. When the buoyancy force becomes the dominant force driving the air movement in the room, a full or nearly full thermal stratification could be achieved, which was the case for the DSD. A more stratified

temperature field implies a more efficient heat removal by an air supply device.

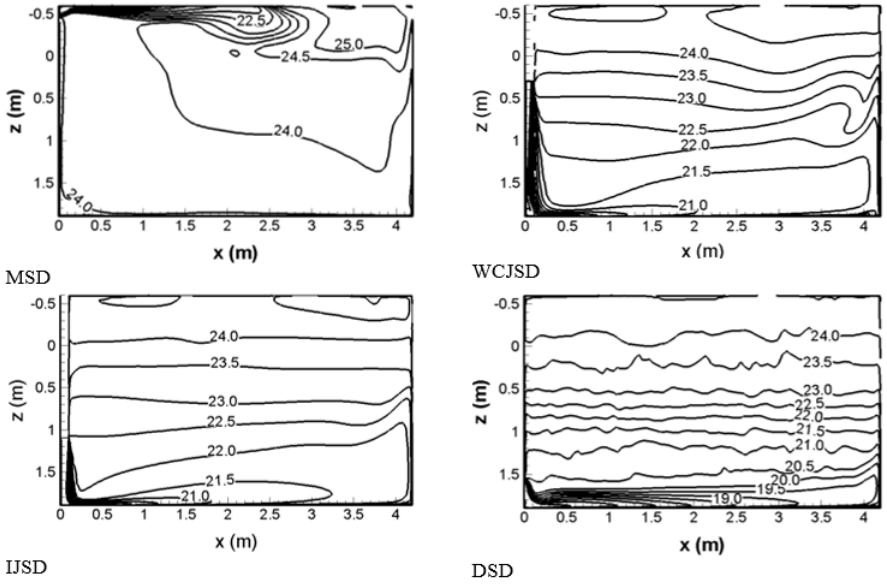

Figure 17. Vertical temperature distributions for (a) MSD, (b) WCJSD, (c) IJSD and (d) DSD.

In Paper IV the flow behavior close to the WCJSD was more closely investigated by using smoke visualization and infrared camera. The WCJSD used in this paper was a corner-mounted supply device, i.e., a supply device in each of the corners in the open-plan office. Figure 18 shows the flow path for the corner-mounted WCJSD.

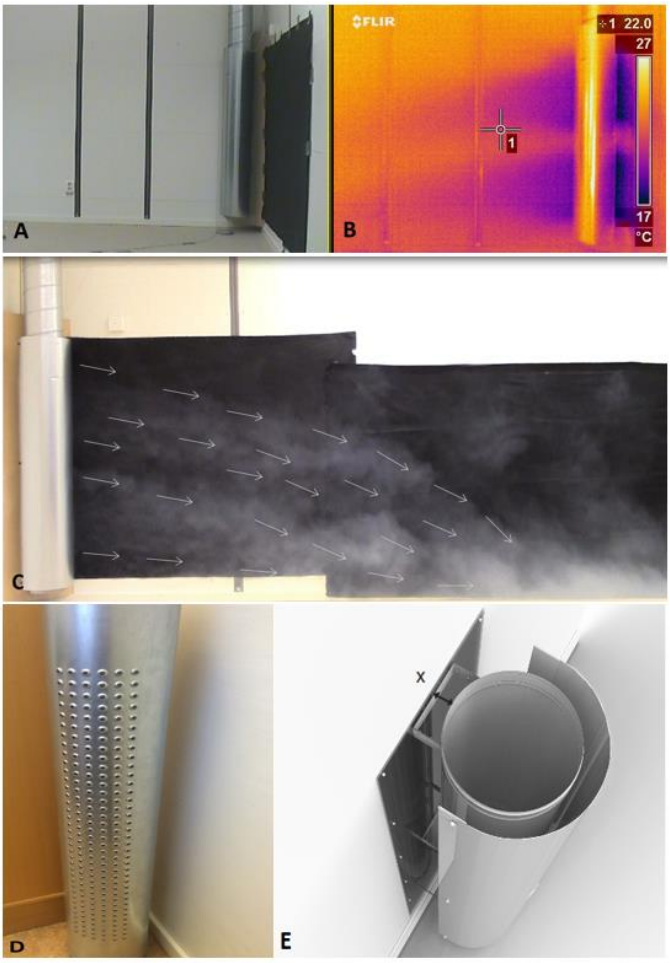

Figure 18. (A) Confluent jet supply diffuser blowing towards the corner, (B) Supply flow pattern visualized by infrared photo, (C) Supply flow pattern visualized by smoke, (D) Perforated side of the Confluent diffuser and (E) Top view of the Confluent diffuser in practice (perforated side towards wall).

As the distance from the diffuser increases, the effect of the momentum becomes less important and the impact of buoyancy force increases instead, see Figure 18. According to the observation from smoke visualization in the room and analyzing the data for temperature and velocity distribution, two situations were categorized at the end of the jet path on the wall. When the distance between opposite diffusers was not large enough and no obstacles disturbed the wall jet, the two

jets met each other and collided. In the collision region, the direction of the two jets was mostly downward and towards the floor. Smoke visualization in the room showed that the new resultant jet spread through the room not only laterally over the floor but also over the floor.

5.2.2 Energy performance

Paper III compares the ventilation performance of four air supply devices in terms of thermal removal efficiency (ε_t) at three heat loads, and temperatures in the occupied zone. The exhaust temperatures for all supply devices were designed to be 24.3°C in energy balance calculations, and to achieve that, cooling is provided by a chilled ceiling in all cases. At the lowest heat load, there is a significant difference between the MSD and the stratified devices with regards to the temperatures in the occupied zone, see Figure 19. The mixing supply device (MSD) provided the highest occupied zone temperature (24.1°C), followed by the impinging jet supply device (IJSD) (22.5°C), wall confluent jet supply device (WCJSD) (22.3°C), and displacement supply device (DSD) (21.6°C). When the heat load increases from 17 to 51 W/m^2 the temperatures for WCJSD, IJSD and DSD increase and approach the temperature for MSD, where the temperatures are more or less constant. One explanation of the constant temperature for MSD is the increased cooling of the chilled ceiling; the ceiling cools the air coming from the device.

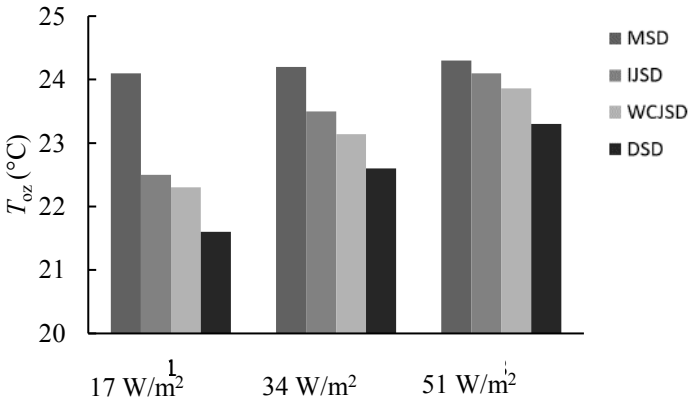

Figure 19. Temperatures in the occupied zone.

In Paper III a comparison of ventilation performance at the same occupied zone temperature has also been made. The temperature in the occupied zone is set to 24.2°C for the four devices. The temperature remained constant with different heat loads or different supply flow rates. The results are shown in Table 5.

Table 5. Comparison of cooling capacity.

Supply device	Heat load (W/m^2)	Difference of cooling capacity[1] (W)	Increased cooling capacity[1] (-)
MSD	34.0	—	—
IJSD	35.5	23	4%
WCJSD	36.4	36	7%
DSD	38.0	60	12%

[1] Compared with the MSD based on a floor area of 15.12 m^2 (W).

Table 6 compares the air-flow rate as well as fan power required for each supply device for achieving the same occupied zone temperature, at the heat load of 34 W/m^2 and with the same supply air temperature of 16°C. The DSD required the lowest air-flow rate of 0.0208 m^3/s among the four devices. WCJSD and IJSD require 1.06 and 1.09 more flowrates respectively than DSD. The MSD required 1.2 times higher air-flow rate and needed 1.74 times higher fan power than the DSD, by using the relations between the flow rate, Q, pressure difference, Δp, and the fan power, E, i.e., $\Delta p \propto Q^2$, $E \propto Q^3$ (Karimipanah, Awbi and Moshfegh, 2008). The WCJSD and IJSD, required 1.06 and 1.09 times higher air-flow rate respectively, which corresponds to 1.18 and 1.32 times more fan power but was still less compared with the MSD.

Table 6. Performance in terms of fan power.

Supply device	Supply air-flow rate (m^3/s)	Air-flow ratio [1]	Fan power ratio[1]
MSD	0.025	1.2	174%
IJSD	0.0228	1.09	132%
WCJSD	0.022	1.06	118%
DSD	0.0208	—	—

[1] Compared with the DSD.

In Paper V a comparison of three different devices has been performed by measurements. The devices used were mixing supply

device (MSD), wall confluent jet supply device (WCJSD) and displacement supply device (DSD). Temperatures were measured in the occupied zone for three different supply temperatures. The result is shown in Table 7.

Table 7. The influence of supply air device on the mean air temperature in the occupied zone.

Case	T_{supply} (°C)	T_{mean} (°C)	ΔT (°C)
WCJSD	14	23.9	-
DSD	14	24.1	+0.2
MSD	14	24.4	+0.5
WCJSD	16	24.3	-
DSD	16	24.5	+0.2
MSD	16	25.6	+1.3
WCJSD	18	24.0	-
DSD	18	24.2	+0.2
MSD	18	26.4	+2.4

The results show that the WCJSD provides 0.2°C lower air temperature in the occupied zone compared to the system using DSD. Comparison between WCJSD and MSD shows a considerably greater difference. The differences vary between 0.5°C to 2.4°C. Thus, the confluent jet ventilation systems provide better cooling of the occupied zone at the same supply air temperature and flow rate. The lower temperature in the occupied zone for confluent jets compared to the other systems indicates that a good stratification is reached within this zone.

5.2.3 Air change effectiveness

In Paper III the air change effectiveness, ε_a, for four different devices was investigated for a heat load of 17 W/m^2. As shown in Figure 20, the DSD provided the highest value of ε_a with the MSD having a value greater than 0.5 compared to perfect mixing, due to certain stratifications created within the room. WCJSD and IJSD have values close to each other, they provides better ε_a than MSD but lower than DSD.

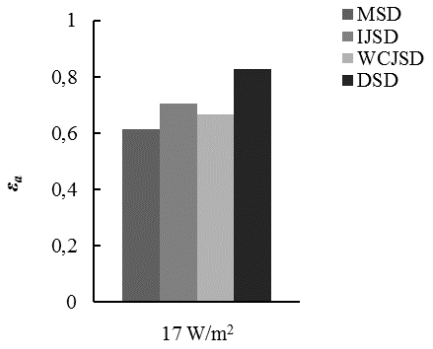

Figure 20. Comparison of air change effectiveness.

Paper IV is an experimental investigation for three different devices in an open-plan office: an under-floor device (UFAD), a wall confluent jet supply device (WCJSD) and a mixing supply device (MSD). Both UFAD and WCJSD are considered to be stratified air distribution systems. Table 8 shows the local mean age of air at a height of 1.2 m at nine positions in the room including the exhaust; the air exchange efficiency for the room is also shown. The measurements are performed for two cases, *A* and *B*, *B* has higher heat load and supply airflow than *A*. The lowest air exchange efficiency is for the ceiling-mounted MSD and the highest is for the UFAD. The corner-mounted WCJSD also produced slightly higher air exchange efficiency than MSD but slightly lower than for the UFAD. The lower local mean age of air for the majority of measuring points for UFAD and WCJSD are an indicator of well-ventilated zones. The higher local mean age of air for the MSD case is consistent with the lower air exchange efficiency for this air supply method.

Table 8. Local mean age of air and air exchange efficiency.

Ventilation strategy		UFAD				WCJSD		MSD	
Case		Straight-grill		Curved-grill		*A*	*B*	*A*	*B*
		A	*B*	*A*	*B*				
Local mean age of air [min]	Point 1	9.9	5.3	8.6	5.4	9.9	6.9	10.0	7.5
	Point 2	10.1	6.2	9.1	8.4	9.7	7.0	10.1	7.0
	Point 3	9.4	2.6	13.5	7.0	10.3	7.4	10.5	7.0
	Point 4	5.7	5.1	4.9	3.9	8.9	6.1	9.9	7.6
	Point 5	6.4	5.1	7.0	6.4	9.4	6.1	10.1	7.3
	Point 6	6.9	5.1	8.0	6.3	9.4	5.9	10.8	7.1
	Point 7	5.6	4.5	4.5	3.5	8.2	5.9	10.1	7.5
	Point 8	6.5	5.0	6.6	5.8	9.1	6.3	10.2	7.3
	Point 9	6.7	3.7	6.2	6.0	9.0	6.4	10.5	7.2
	Exhaust	9.6	7.1	9.9	7.5	10.7	7.6	11.0	7.7
Air exchange efficiency [%]		64	61	63	60	55	57	52	51

Paper V and VII give a comparison of three different air supply devices including a wall confluent jet supply device (WCJSD), displacement supply device (DSD) and a mixing supply device (MSD). For the three devices the local mean age of air (MAA) and air exchange efficiency were measured using tracer gas measurements. Cases 1, 7 and 10 have the same boundary conditions, and Cases 4, 8 and 11 also have the same boundary conditions. The WCJSD was positioned at two heights, 1.7 m and 2.2 m. Table 9 below shows that the WCJSD placed at 2.2 m provides the highest value of ε_a, which is 50–52%, followed by the DSD (50%) and the MSD provides 47%. WCJSD at 1.7 m obtains results similar to the system with MSD in terms of air change efficiency. The results show a very small difference in ventilation efficiency between the different systems and in theory there should have been a larger difference.

Table 9. Results of local mean age of air and air exchange efficiency (ε_a).

Ventilation system	Position	Case	C_0	Mean age air (min)	Local air change index (%)$_0$	
WCJSD @2.2 m	0.1 m	4	407.94	19.5	104.4	
		1	252.89	24.6	98.3	
	1.2 m	4	394.66	20.1	101.4	
		1	264.29	24.6	98.3	
	1.7 m	4	360.44	19.4	105.0	
		1	225.38	24.1	100.3	
	Outlet	4	411.85	20.4	52.3	ε_a
		1	407.94	24.2	50.1	
WCJSD @1.7 m	0.1 m	4	204	18.3	98.2	
		1	202.88	24.4	103.3	
	1.2 m	4	249.2	17.4	103.3	
		1	237.75	25.3	99.4	
	1.7 m	4	214.95	17.6	102.1	
		1	233.01	23.5	106.9	
	Outlet	4	216.26	18.0	47.0	ε_a
		1	225.73	25.2	47.5	
DSD	0.1 m	8	249.55	14.6	108.1	
		7	189.88	8.3	193.9	
	1.2 m	8	258.02	16.4	108.1	
		7	260.87	19.4	83.5	
	1.7 m	8	237.71	15.8	100.1	
		7	243.98	17.1	94.4	
	Outlet	8	235.09	15.8	49.6	ε_a
		7	239.11	16.2	50.5	
MSD	0.1 m	11	314.39	28.0	101.7	
		10	294.18	34.2	100.0	
	1.2 m	11	262.01	28.0	101.8	
		10	253.51	33.2	103.1	
	1.7 m	11	215.63	30.7	92.9	
		10	281.36	32.4	105.8	
	Outlet	11	263.97	28.5	47.6	ε_a
		10	272.85	34.2	47.6	

WCJSD mounted at different heights shows small differences but differences are bigger for higher airflow rates. DSD has the youngest air in all cases and at all heights but for higher airflow rates the MAA

for DSD approaches the MAA for WCJSD. However, the MAA for MSD is much higher than for DSD and WCJSD in all cases.

In Paper VI a numerical investigation of air change effectiveness in an office room ventilated by an IJSD has been more closely investigated. Five cases of simulation were carried out to investigate the effects of chilled ceiling cooling power, heat load composition as well as its location, and supplied air conditions on IJSD performance in an office room. Case 1 used only one occupant as a heat load. In Case 2 heat loads such as a computer and lights were added, while Cases 3 and 4 included external heat loads due to solar radiation on floor and heat transfer on window. Case 5 is similar to Case 3 but one more occupant was added to the room. Figure 21 shows the air change effectiveness, the one on the left side represents a vertical cross section 2.1 m from the device and the one on the right side is a horizontal view at a level of 1.1 m (breathing zone) from the floor.

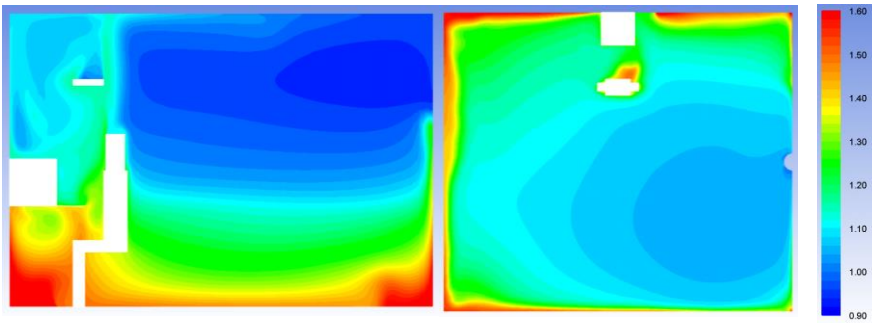

Figure 21. Air change effectiveness for case 2.

The flow pattern in the room turns against the working place because of the higher buoyancy effect generated from the heat sources; this behavior reduces the local mean age of air for the zone around the person. The right corner at the opposite wall from the inlet device shows a lower mean age of air than the left corner on the same wall confirming that the flow turns against the workstation. For more figures on the rest of the cases considered see the paper.

For all five cases the average mean age of air near the surface of the occupants are well below the nominal time constant (which is equal to MAA at the exhaust), see Table 10. The nominal time constant for Case

1 is 3760 s and for the other four Cases 1635 s. Case 2 provides the best air quality around the occupant. The results also indicate that Case 5 provides the same level of air quality (if neglecting contaminants from occupants) as Case 3.

Table 10. Area weighted average of MAA over the occupants' surface.

	Case 1	Case 2	Case 3	Case 4	Case 5
Person 1	3057 s	1141 s	1258 s	1348 s	1285 s
Person 2	N/A	N/A	N/A	N/A	1287 s

5.3 Research question #3

Research question #3 focuses on the thermal comfort for different supply devices based on stratified ventilation. Paper III represents numerical calculations for the ventilation performance of four different supply devices for an office environment, including with a focus on the thermal comfort.

The overall thermal comfort was assessed using PPD index as a direct reflection of the occupied zone temperature, i.e., the less appropriate the room temperature, either (too) warm or (too) cool, the greater the values of PPD. Based on figure 22, it could be seen that the thermal environment of the small office for most cases was acceptable, as PPD values were controlled well below the threshold of 10% for thermal comfort (International Organization for Standardization, 2005). However, this was not the case for the DSD at the lowest heat load of 17 W/m^2, because the PPD value exceeded the permitted level. A Higher air supply temperature would be used to remedy this condition, especially for situations where incoming solar radiation is not considered on the floor.

Local thermal discomfort is another important aspect for evaluating ventilation performance. In this study, draft discomfort was assessed at a height of 0.1 m above the floor, as recommended by ASHRAE (2004) and International Organization for Standardization (2005). Figure 22 showed plots of the average DR within the occupied zone at this height. The MSD investigated in this study had the highest average value of DR (about 18%), followed by the WCJSD and IJSD (about 12%), and

DSD (about 9%). For four devices, the draft risks at a height of 0.1 m might not be critical as the average values of DR were lower than 20%. It is worth mentioning that even with the high DR values generated by the MSD near the floor level, it might not cause problems in regions close to the occupant, because buoyancy from the internal heat sources tended to direct the supplied flow to the opposite side of the room.

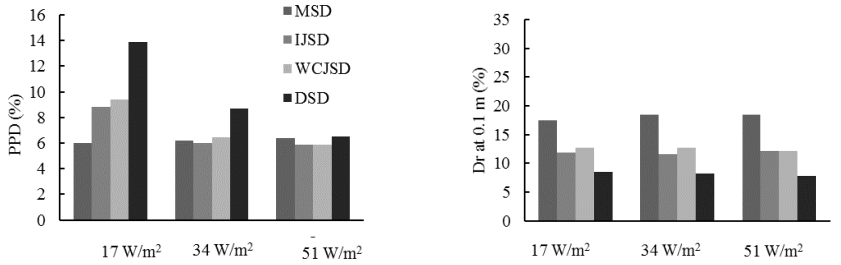

Figure 22. PPD in the occupied zone and the draft at the height of 0.1 m for three different heat loads.

Constant heat load and supply device airflow but a change in the temperature of the inlet air results in a decreasing of the DR for all the devices, see Figure 23.

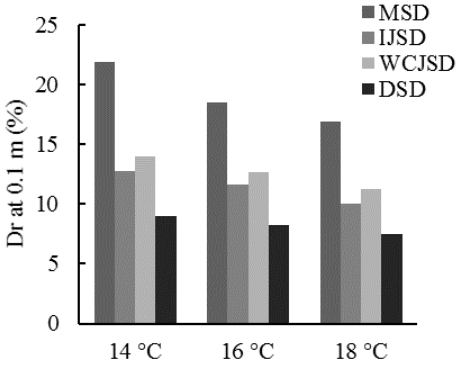

Figure 23. DR for different supply temperatures.

Under identical conditions, the results indicated that WCJSD and IJSD behaved like a combined mixing and displacement system: they could provide an acceptable thermal environment, while removing excess heat more efficiently as compared to the conventional mixing system.

Paper IV considers three types of air supply devices, namely WCJSD and UFAD with straight and curved vanes. The main purpose of this paper was to evaluate the performance of these supply devices in terms of their ability of heat removal, thermal comfort, local mean age of air and air exchange efficiency provision for the conditioned space. The study object is an open-plan office, see Paper IV for more information about the setup.

Tables 11, 12 and 13 show the results of the thermal comfort measurements performed for two different cases, *A* and *B*; Case *B* has a higher heat load and higher airflow from the inlet devices than Case *A*. The measurement points for the thermal comfort parameters were chosen in areas close to the occupants and at 1.2 m above the floor.

Table 11. Thermal comfort indices for UFAD supply devices.

Case	GT	MP	Indoor Air Properties		Thermal Comfort Indices				
			T (°C)	v_a (m/s)	DR (%)	T_{eq} (°C)	PMV	PPD	RH (%)
A	ST	4	23.9	0.1	9.4	23.6	0.1	5.3	27.6
		13	23.7	0.1	9.0	23.5	0.0	5.1	21.2
		7	23.9	0.1	4.5	23.9	0.1	5.5	27.2
		12	23.8	0.0	0.3	23.8	0.1	5.2	23.2
	CU	4	23.9	0.1	8.6	23.7	0.0	5.1	19.4
		13	23.4	0.0	0.9	23.4	0.0	5.0	19.6
		7	23.8	0.1	8.0	23.5	0.0	5.1	21.1
		12	23.3	0.0	1.6	23.3	0.0	5.0	20.2
B	ST	4	24.4	0.1	7.4	24.2	0.5	9.6	62.1
		13	23.9	0.0	0.5	23.9	0.3	7.4	55.8
		7	24.5	0.1	10.3	24.1	0.4	9.3	62.6
		12	23.9	0.1	6.3	23.8	0.3	7.6	59.7
	CU	4	24.2	0.1	9.8	23.9	0.3	6.7	44.8
		13	23.9	0.0	4.2	23.8	0.4	8.0	63.1
		7	24.3	0.1	5.8	24.1	0.3	7.5	46.7
		12	24.2	0.0	1.3	24.2	0.4	9.1	57.8

GT: Grill Type, ST: Straight, CU: Curved, MP: Measuring point, T: Air temperature, v_a: Air velocity, DR: Draught Rating, T_{eq}: Equivalent temperature, PMV: Predicted Mean Vote, PPD: Predicted Percentage of Dissatisfied, RH: Relative Humidity

The air distribution system has a major impact on the flow pattern and changing grills have an effect of the ventilation effectiveness. However, both grill types behaved similarly in terms of fulfilling the ISO standard requirements for thermal comfort.

Table 12. Thermal comfort indices for WCJSD.

Case	MP	Indoor Air Properties		Thermal Comfort Indices				
		T (°C)	v_a (m/s)	DR (%)	T_{eq} (°C)	PMV	PPD	RH (%)
A	4	24.5	0.1	10.6	24.1	0.2	5.7	20.0
	13	24.1	0.1	10.5	23.7	0.1	5.3	19.3
	7	24.0	0.2	26.5	23.2	-0.1	5.6	20.9
	11	24.7	0.2	15.4	24.0	0.1	5.6	20.0
	12	24.7	0.2	15.4	24.0	0.1	5.6	20.0
B	4	24.5	0.1	11.6	24.1	0.2	5.8	21.0
	7	23.9	0.2	30.1	22.9	-0.1	5.9	28.1
	11	25.0	0.1	11.1	24.6	0.3	6.6	19.2
	12	23.5	0.3	49.8	22.1	-0.3	7.9	21.5

MP: Measuring point, T: Air temperature, v_a: Air velocity, DR: Draught Rating, T_{eq}: Equivalent temperature, PMV: Predicted Mean Vote, PPD: Predicted Percentage of Dissatisfied, RH: Relative Humidity

With WCJSD installed at the corners of the room, draft rates were in the range of category C (DR < 25%) but PPD indices are in category A (< 6%) and PMV indices are also in Category A (–0.2 < PMV < +0.2) which implies that they are totally in agreement with the best category of ISO standard, see International Organization for Standardization (2005).

For a mixing system, besides a homogenous temperature distribution, there is higher tendency for more draft in occupied zone. In this case, the draft and inadequate temperature distributions in the occupied zone could be more prevalent if a mixing system is used for open-plan offices. It is concluded that UFAD and corner-mounted WCJSD are more suitable than MSD for use in open-plan office environment.

Table 13. Thermal comfort indices for MSD.

Case	MP	Indoor Air Properties		Thermal Comfort Indices				
		T (°C)	v_a (m/s)	DR (%)	T_{eq} (°C)	PMV	PPD	RH (%)
A	4	25.7	0.1	8.9	25.2	0.5	10.7	31.7
	13	24.9	0.1	11.0	24.4	0.3	7.4	33.6
	7	25.7	0.1	11.0	25.3	0.5	11.2	33.3
	12	25.2	0.1	8.7	24.9	0.4	9.1	34.1
B	4	26.2	0.2	15.8	25.5	0.5	10.0	18.2
	13	25.0	0.1	11.8	24.5	0.3	6.5	19.6
	7	25.9	0.1	6.9	25.7	0.5	10.8	18.1
	12	25.1	0.1	9.9	24.7	0.3	7.0	18.8

MP: Measuring point, T: Air temperature, v_a: Air velocity, DR: Draught Rating, T_{eq}: Equivalent temperature, PMV: Predicted Mean Vote, PPD: Predicted Percentage of Dissatisfied, RH: Relative Humidity

In Paper VII the aim of the experimental study was the thermal comfort (PMV and PPD) of three different ventilation supply devices, i.e., mixing supply device (MSD), displacement supply device (DSD) and wall confluent jet supply device (WCJSD), in an office room.

Figure 24 compares the PMV for different supply devices for different boundary conditions and at different heights in the room. PMV for all six positions in the room were presented, and the median value is also shown. PMV for DSD is lower in every case and at all heights than the other supply devices.

At a height of 0.1 m the value is always below the neutral value (0). The value for WCJSD is close to the DSD value at 0.1 m but always above the neutral value. There is also a tendency that MSD in all cases has a higher PMV for WCJSD and DSD. At the higher airflow rates this tendency is rather strong.

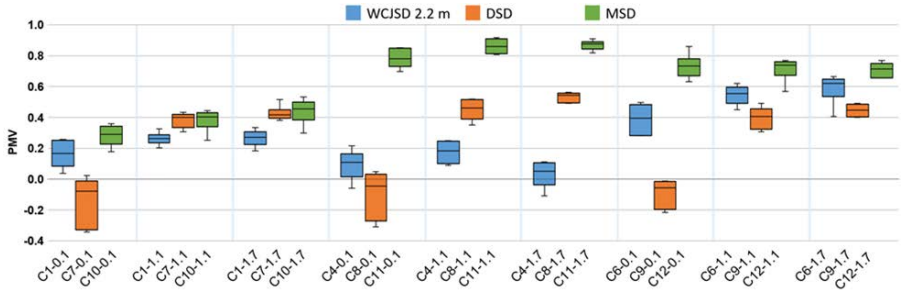

Figure 24. PMV for different cases.

Figure 25 compares the PPD for different supply devices at different boundary conditions and at different heights in the room. PPD for all six positions in the room is presented and the median value is shown. There are small differences between the supply devices at 20 l/s but at higher flows and especially at 25 l/s there is a big difference. WCJSD shows the lowest value and best comfort in most of the cases.

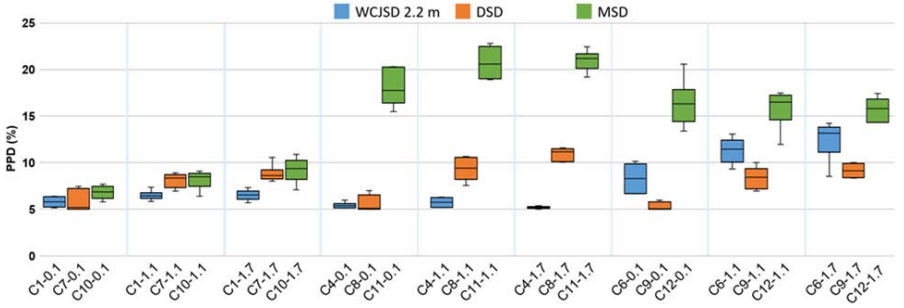

Figure 25. PPD for different cases.

The comparison of PMV and PPD between the three supply devices shows that MSD provides poorer comfort than DSD and WCJSD. DSD and WCJSD have more or less the same thermal comfort performance.

6 Conclusions

This chapter covers the conclusions presented in the appended papers in relation to the research questions presented in Section 1.4.

The location of displacement supply device with respect to windows in a cold climate has significant effect on the flow pattern below the window by pushing the downdraft towards the opposite wall. In the present case the velocity from the downdraft from a well-insulated window decreases by approximately 9.5% if the airflow from the supply device increases from 10 l/s to 15 l/s. Different supply airflow rates also have an effect on the temperature of the downdraft. The downdraft temperature decreases by approximately 0.5°C with the higher airflow rate. The thermal insulation of the window also has a vital effect on the downdraft; windows with lower thermal performance will increase the strength of the downdraft from the window. As a result, well-insulated windows enable alternative heating systems like the one studied in the present study, i.e., floor heating.

The difference in the airflow patterns between the different air supply systems was essentially related to the characteristics of the air supply devices, such as type, configuration and position, as well as air supply velocities and momentum. For WCJSD, IJSD and DSD, the position of heat sources (i.e., occupant, etc.) played an important role in formation of the room airflow pattern. This is due to the fact that heat sources tended to create buoyancy flows but also other obstacles like furniture, etc. have a major influence on the airflow in the room. The airflow from the MSD is less influenced by the heat sources because of its high momentum.

Vertical temperature distribution in the different offices shows that IJSD and WCJSD produce similar results, both is showing a clear stratification of the air in the room. It is worth mentioning that the only remarkable difference is the lower air temperature close to the floor for the WCJSD compared to IJSD at the end of the room. DSD also shows a strong stratification of the air in the room but has a stronger temperature gradient than IJSD and WCJSD, especially close to the floor. MSD has a uniform temperature distribution; the only temperature gradient is close to the ceiling. One interesting observation is that the temperature in the occupied zone is lower and a more

stratified temperature field implies a more efficient heat removal by a stratified air supply device. The results in Paper III reveal that IJSD has an average occupied zone temperature of 22.5°C, WCJSD 22.3°C and DSD 21.6°C. MSD provided the highest occupied zone temperature of 24.1°C. In terms of energy saving (fan power) for the same temperature in the occupied zone, it is shown that DSD has the lowest energy use, WCJSD is 18% higher, IJSD is 32% higher and MSD has highest energy use, 74% more than DSD.

The results confirm that the air change effectiveness (ACE) in all the papers for the DSD, WCJSD and IJSD is close to each other. However, MSD produces the lowest ACE compared to IJSD, WCJSD and DSD. Local mean age of air shows that DSD has the youngest air in the occupied zone, especially at lower heights; WCJSD and IJSD have considerably younger air in the occupied zone compared to MSD. However, the location and the size of the heat sources, have major impact on the local mean age of air.

The thermal comfort has been investigated by considering PPD, PMV and DR (draft) indexes. In Paper III, PPD for DSD is higher compared to IJSD and WCJSD (they are almost on the same level), however, MSD is lower than all the stratified devices. However, by increasing the heat load in the room the difference between the stratified supply devices was diminished. In the same paper, DR for the DSD is lowest and for MSD highest, with IJSD and WCJSD in the middle of these. However, increasing the heat load had almost no impact on DR. BY increasing the temperature of the supply air DR decreases. Paper VII reveals that, with a relative high heat load, the supply air flowrate has a significant effect on the PPD and PMV, especially on MSD, which in this case has much higher PPD than DSD and WCJSD.

7 Future Studies

In this thesis, only office space has been considered as study objects. An extension of this work would be to investigate the performance of the supply devices in other indoor environments. Supply devices investigated in this study such as IJSD and WCJSD are expected to be able to transport fresh air further into the room, and this should be useful in larger spaces, such as industrial premises, shopping centers, and auditoriums. Another limitation in this work was that all measurements were performed in the laboratory environment; certainly full-scale measurements have been carried out but with well-defined boundary conditions. Investigation of the performance of supply devices in "real" environments would be troublesome and challenging; the biggest advantage would be that in addition to technical findings on the indoor environment, the occupants could also participate through surveys. However, in order to fully evaluate the studied supply devices, measurements in the real environment should be performed. Some contacts with a property owner have been made where measurements in large office landscapes, significantly larger than those included in this work, will be performed.

One topic for the present study was to investigate the interaction between downdraft and airflow from the inlet supply device. The limitation was that only airflow from a DSD was investigated. It would be interesting in a future work to compare how airflow from different stratified supply devices, such as IJSD and WCJSD, interact with downdraft from windows. There are studies that claim that IJSD and WCJSD can also be used for heating, and it would be interesting to do analyze on the above topic for both cooling and heating cases.

Another topic for the current work was to investigation the air change effectiveness in a room with an IJSD. All cases have been designed for the cooling case. A future interesting study is to investigate the influence of a heating case on the air change effectiveness in a room equipped with an IJSD.

An additional difficulty that has been revealed during the work of this thesis was to measure the ventilation efficiency with the trace gas measurements. The trace gas method is appropriate when the room air is mixed and not stratified. When stratified systems are under

consideration, it is important to measure in vicinity of the occupants. This effect has been confirmed in the numerical simulations that there is a clearer difference between air change efficiency for stratified systems compared to mixing systems. The purpose of a stratifying system is to hand over where the occupants are and then measuring outside this zone gives an incorrect picture. Therefore, in a future work it is important to clarify the consequences and propose a method to improve it.

References

Al Ali, A. R. and Janajreh, I. (2015) 'Numerical simulation of turbine blade cooling via jet impingement', *Energy Procedia*. Elsevier, 75, pp. 3220–3229.

Anger, N. and Zannier, L. (2017) 'A new era of EU energy policy? Delivering on the Energy Union by National Plans. CEPS Commentary, 6 June 2017'.

ASHRAE, A. (2004) 'Standard 55-2004, thermal environmental conditions for human occupancy, atlanta: american society of heating, refrigerating, and air-conditioning engineers', *Inc., USA*.

Awbi, H. B. (2003) *Ventilation of buildings*. Taylor & Francis.

Awbi, H. B. (2008) *Ventilation systems: design and performance*. Psychology Press.

Awbi, H. B. (2011) 'Energy efficient ventilation for retrofit buildings', in *Proceedings of 48th AiCARR international conference on energy performance of existing buildings*, p. e23.

Brunsgaard, C. *et al.* (2012) 'Evaluation of the indoor environment of comfort houses: Qualitative and quantitative approaches', *Indoor and Built Environment*. Sage Publications Sage UK: London, England, 21(3), pp. 432–451.

Bruun, H. H. (1995) 'Hot-wire anemometry-principles and signal analysis'. Oxford science publications.

Cao, G. *et al.* (2014) 'A review of the performance of different ventilation and airflow distribution systems in buildings', *Building and Environment*. Elsevier, 73, pp. 171–186.

Cehlin, M. and Moshfegh, B. (2010) 'Numerical modeling of a complex diffuser in a room with displacement ventilation', *Building and Environment*. Elsevier, 45(10), pp. 2240–2252.

Cehlin, M., Moshfegh, B. and Stymne, H. (2000) 'Mapping of Indoor Climate Parameters in Volvo, Eskilstuna'. University of Gävle.

Chen, H. J., Moshfegh, B. and Cehlin, M. (2012) 'Numerical investigation of the flow behavior of an isothermal impinging jet in a room', *Building and Environment*. Elsevier, 49, pp. 154–166.

Chen, H. J., Moshfegh, B. and Cehlin, M. (2013) 'Investigation on the flow and thermal behavior of impinging jet ventilation systems in an office with different heat loads', *Building and Environment*. Elsevier, 59, pp. 127–144.

Cho, Y., Awbi, H. B. and Karimipanah, T. (2002) 'A comparison between four different ventilation systems', in *Proceedings of the 8th International Conference on Air Distribution in Rooms (Roomvent 2002)*, pp. 181–184.

Cho, Y., Awbi, H. B. and Karimipanah, T. (2005) 'Comparison between wall confluent jets and displacement ventilation in aspect of the spreading rate on the floor'.

Cho, Y., Awbi, H. B. and Karimipanah, T. (2008) 'Theoretical and experimental investigation of wall confluent jets ventilation and comparison with wall displacement ventilation', *Building and Environment*. Elsevier, 43(6), pp. 1091–1100.

Cowell, T. . and Heikel, M. . (1988) 'The calibration of constant temperature hot-wire anemometer probes at low velocities', in *Second UK National Conf. On Heat Transfer*. Strathclyde, UK: University of Strathclyde, pp. 1607–1622.

Durbin, P. A. (1995) 'Separated flow computations with the k-epsilon-v-squared model', *AIAA journal*, 33(4), pp. 659–664.

Etheridge, D. W. and Sandberg, M. (1996) *Building ventilation: theory and measurement*. John Wiley & Sons Chichester.

Fanger, P. O. (1967) 'Calculation of thermal comfort, Introduction of a basic comfort equation', *ASHRAE transactions*, 73(2), p. III-4.

Fanger, P. O. (1970) 'Thermal comfort. Analysis and applications in environmental engineering.', *Thermal comfort. Analysis and applications in environmental engineering.* Copenhagen: Danish Technical Press.

Fanger, P. O. (1977) ‘Discomfort due to air velocities in spaces’, in *Proc. of Meeting of Commission B1, B2, E1, of Instit. Refrig.*, pp. 289–296.

Fanger, P. O. *et al.* (1988) ‘Air turbulence and sensation of draught’, *Energy and buildings*. Elsevier, 12(1), pp. 21–39.

Fanger, P. O., Højbjerre, J. and Thomsen, J. O. B. (1974) ‘Thermal comfort conditions in the morning and in the evening’, *International journal of biometeorology*. Springer, 18(1), pp. 16–22.

Fisk, W. J. and Rosenfeld, A. H. (1997) ‘Estimates of improved productivity and health from better indoor environments’, *Indoor air*. Wiley Online Library, 7(3), pp. 158–172.

Fluent, A. (2010) ‘13.0 User’s Guide,(2010)’, *Ansys Inc*.

Gan, G. and Awbi, H. B. (1994) ‘Numerical simulation of the indoor environment’, *Building and Environment*. Elsevier, 29(4), pp. 449–459.

Ghahremanian, S. and Moshfegh, B. (2014) ‘A Study on Proximal Region of Low Reynolds Confluent JetsPart 2: Numerical Prediction of the Flow Field’, *ASHRAE Transactions*. American Society of Heating, Refrigeration and Air Conditioning Engineers, Inc., 120, p. 271.

Heiselberg, P. (1994) ‘Draught risk from cold vertical surfaces’, *Building and Environment*. Elsevier, 29(3), pp. 297–301.

Hu, S., Chen, Q. and Glicksman, L. R. (1999) ‘Comparison of energy consumption between displacement and mixing ventilation systems for different US buildings and climates’, *ASHRAE Transactions*. American Society of Heating, Refrigeration and Air Conditioning Engineers, Inc., 105, p. 453.

Jaakkola, J. J. K., Heinonen, O. P. and Seppänen, O. (1989) ‘Sick building syndrome, sensation of dryness and thermal comfort in relation to room temperature in an office building: need for individual control of temperature’, *Environment international*. Elsevier, 15(1–6), pp. 163–168.

Jahedi, M. and Moshfegh, B. (2017) 'Experimental study of quenching process on a rotating hollow cylinder by one row of impinging jets', in *Experimental Heat Transfer, Fluid Mechanics and Thermodynamics*.

Janbakhsh, S. and Moshfegh, B. (2014) 'Numerical study of a ventilation system based on wall confluent jets', *HVAC&R Research*. Taylor & Francis, 20(8), pp. 846–861.

Janbakhsh, S. and Moshfegh, B. (2015) 'Investigation of design parameters for an air supply device based on wall confluent jets'.

Jones, W. P. and Launder, Be. (1972) 'The prediction of laminarization with a two-equation model of turbulence', *International journal of heat and mass transfer*. Elsevier, 15(2), pp. 301–314.

Jonsson, B. (1985) *Heat transfer through windows during the hours of darkness with the effect of infiltration ignored*. Statens Raad foer Byggnadsforskning, Stockholm (Sweden).

Kabanshi, A. (2016) 'Experimental Evaluation of Intermittent Air Jet Ventilation Strategy: Cooling Effect Analysis', *Proceedings, IAQVEC 2016, Songdo, Republic of Korea*.

Kabanshi, A., Wigö, H. and Sandberg, M. (2016) 'Experimental evaluation of an intermittent air supply system–Part 1: Thermal comfort and ventilation efficiency measurements', *Building and Environment*. Elsevier, 95, pp. 240–250.

Karimipanah, T. *et al.* (2007) 'Investigation of air quality, comfort parameters and effectiveness for two floor-level air supply systems in classrooms', *Building and Environment*. Elsevier, 42(2), pp. 647–655.

Karimipanah, T. and Awbi, H. B. (2002) 'Theoretical and experimental investigation of impinging jet ventilation and comparison with wall displacement ventilation', *Building and Environment*. Elsevier, 37(12), pp. 1329–1342.

Karimipanah, T., HB, A. and Moshfegh, B. (2008) 'The air distribution index as an indicator for energy consumption and performance of ventilation systems', *Journal of the Human-Environment System*. Japanese Society of Human-Environment System, 11(2), pp. 77–84.

Knight, K. J. *et al.* (2005) ‘Practical application of the LES method to mixing in large indoor spaces’, in *ASME 2005 International Mechanical Engineering Congress and Exposition*. American Society of Mechanical Engineers, pp. 587–594.

Kobayashi, T. *et al.* (2017) ‘Numerical investigation and accuracy verification of indoor environment for an impinging jet ventilated room using computational fluid dynamics’, *Building and Environment*. Elsevier, 115, pp. 251–268.

Larraona, G. S. *et al.* (2013) ‘Computational parametric study of an impinging jet in a cross-flow configuration for electronics cooling applications’, *Applied Thermal Engineering*. Elsevier, 52(2), pp. 428–438.

Launder, B. E., Reece, G. J. and Rodi, W. (1975) ‘Progress in the development of a Reynolds-stress turbulence closure’, *Journal of fluid mechanics*. Cambridge University Press, 68(3), pp. 537–566.

Liu, L., Rohdin, P. and Moshfegh, B. (2015) ‘Evaluating indoor environment of a retrofitted multi-family building with improved energy performance in Sweden’, *Energy and Buildings*. Elsevier, 102, pp. 32–44.

Lundström, H. *et al.* (1990) ‘A microprocessor-based anemometer for low air velocities’, in *Proceedings of Roomvent*, p. 27.

McIntyre, D. A. (1979) ‘The effect of air movement on thermal comfort and sensation’, *Indoor Climate, Danish Building Research Institute, Co penhagen*.

Melikov, A. *et al.* (2005) ‘Field study on occupant comfort and the office thermal environment in rooms with displacement ventilation’, *Indoor air*. Wiley Online Library, 15(3), pp. 205–214.

Melikov, A. K., Langkilde, G. and Derbiszewski, B. (1990) ‘Airflow characteristics in the occupied zone of rooms with displacement ventilation’, *ASHR a E Transactions*, 96(1), pp. 555–563.

Melikov, A. K. and Nielsen, J. B. (1989) 'Local thermal discomfort due to draft and vertical temperature difference in rooms with displacement ventilation', *ASHRAE Transactions (American Society of Heating, Refrigerating and Air-Conditioning Engineers);(USA)*, 95(CONF-890609--).

Mujumdar, A. S. (2014) '15 Impingement Drying', *Handbook of Industrial Drying*. CRC Press, p. 371.

Mundt, E. (1990) 'Convection flows above common heat sources in rooms with displacement ventilation', in *Proceedings of ROOMVENT*, pp. 13–15.

Nielsen, P. V (1974) *Flow in air conditioned rooms: Model eksperiments and numerical solution of the flow equations.*

Nielsen, P. V *et al.* (2005) 'Air Distribution in Rooms Generated by a Textile Terminal--Comparison with Mixing and Displacement Ventilation.', *Ashrae Transactions*, 111(1).

Paul, J. and Steimle, F. (1977) 'New results from measurements with hot-wire anemometers at low velocities and superimposed convection', in *IIF-IIR Commision B1, B2, E1*. Belgrade, Yugoslavia.

Pitchurov, G. *et al.* (2002) 'Field survey of occupants thermal comfort in rooms with displacement ventilation', in *Roomvent 2002*. Technical University of Denmark and Danvak.

Rohdin, P. and Moshfegh, B. (2011) 'Numerical modelling of industrial indoor environments: A comparison between different turbulence models and supply systems supported by field measurements', *Building and Environment*. Elsevier, 46(11), pp. 2365–2374.

Rundström, D. and Moshfegh, B. (2006) 'Investigation of flow and heat transfer of an impinging jet in a cross-flow for cooling of a heated cube', *Journal of electronic packaging*. American Society of Mechanical Engineers, 128(2), pp. 150–156.

Sandberg, M. and Mattsson, M. (1992) 'The effect of moving heat sources upon the stratification in rooms ventilated by displacement ventilation', in *Proc. of the 3rd International Conference on Air Distribution in Rooms*.

SKISTAD, H. (1998) ‘Displacement Ventilation Displacement Ventilation, 1994’, *Journal of Architecture and Planning (Transactions of AIJ)*, 63(507), pp. 27–34.

Skov, P., Valbjørn, O. and Pedersen, B. V (1990) ‘Influence of indoor climate on the sick building syndrome in an office environment’, *Scandinavian journal of work, environment & health*. JSTOR, pp. 363–371.

Standard, I. S. O. (2005) ‘7730: 2005’, *Ergonomics of the thermal environment–Analytical determination and interpretation of thermal comfort using calculation of the PMV and PPD indices and local thermal comfort criteria*.

Standardization, I. O. for (2005) *Ergonomics of the Thermal Environment: Analytical Determination and Interpretation of Thermal Comfort Using Calculation of the PMV and PPD Indices and Local Thermal Comfort Criteria*. International Organization for Standardization.

Wang, M. and Chen, Q. (2010) ‘On a hybrid rans/les approach for indoor airflow modeling (rp-1271)’, *HVAC&R Research*. Taylor & Francis, 16(6), pp. 731–747.

Wargocki, P. *et al.* (1999) ‘Perceived air quality, sick building syndrome (SBS) symptoms and productivity in an office with two different pollution loads’, *Indoor air*. Wiley Online Library, 9(3), pp. 165–179.

Wyon, D. P. (2004) ‘The effects of indoor air quality on performance and productivity’, *Indoor air*. Wiley Online Library, 14(s7), pp. 92–101.

Ye, X. *et al.* (2016) ‘Heating energy consumption of impinging jet ventilation and mixing ventilation in large-height spaces: A comparison study’, *Energy and Buildings*. Elsevier, 130, pp. 697–708.

Zhang, W. and Chen, Q. (2000) ‘Large eddy simulation of indoor airflow with a filtered dynamic subgrid scale model’, *International Journal of Heat and Mass Transfer*. Elsevier, 43(17), pp. 3219–3231.

Appended papers

The papers associated with this thesis have been removed for copyright reasons. For more details about these see:

http://urn.kb.se/resolve?urn=urn:nbn:se:liu:diva-149815